67-FM-29

NATIONAL AERONAUTICS AND SPACE ADMINISTRATION

MSC INTERNAL NOTE NO. 67-FM-29

March 1, 1967

PRELIMINARY MSFN ERROR ANALYSIS FOR AS-504A

By Paul H. Mitchell

Mathematical Physics Branch

FEB LIBRARY RECEIVED INC. NASA STI FACILITY INPUT BRANCH

955 L'Enfant Plaza North, S.W.
Washington, D. C. 20024

OCT 30 1968

MISSION PLANNING AND ANALYSIS DIVISION

MANNED SPACECRAFT CENTER

HOUSTON, TEXAS

(NASA-TM-X-69424) PRELIMINARY MSFN ERROR ANALYSIS FOR AS-504A (NASA) 58 p

N74-71208

Unclas

00/99 16387

MSC INTERNAL NOTE NO. 67-FM-29

PROJECT APOLLO

PRELIMINARY MSFN ERROR ANALYSIS FOR AS-504A

By Paul H. Mitchell
Mathematical Physics Branch

March 1, 1967

MISSION PLANNING AND ANALYSIS DIVISION
NATIONAL AERONAUTICS AND SPACE ADMINISTRATION
MANNED SPACECRAFT CENTER
HOUSTON, TEXAS

Approved: James C. McPherson, Chief
Mathematical Physics Branch

Approved: John P. Mayer, Chief
Mission Planning and Analysis Division

CONTENTS

Section	Page
SUMMARY	1
INTRODUCTION	1
SYMBOLS	2
ERROR MODEL	5
MSFN DESCRIPTION FOR AS-504A	5
DESCRIPTION OF ANALYSIS AND DATA UTILIZATION	6
Earth Parking Orbit Phase	6
Translunar Phase	6
Lunar Parking Orbit Phase	6
LM Operations Phase	7
Transearth Phase	7
ERROR ANALYSIS RESULTS	8
Earth Parking Orbit Phase	9
Translunar Phase	10
Lunar Operations Phase	10
Transearth Phase	11
CONCLUSIONS	11
APPENDIX - COVARIANCE MATRICES	35
REFERENCES	53

TABLES

Table		Page
I	TOPOCENTRIC STATION LOCATION UNCERTAINTIES (1σ) . . .	13
II	DATA CHARACTERISTICS (1σ)	14
III	TRACKING STATIONS VIEW PERIODS	15
IV	SUMMARY OF LOCAL SPACECRAFT NAVIGATIONAL ACCURACIES (3σ) FOR AS-504A	
	(a) RSS Position and Velocity Uncertainties	21
	(b) Uncertainties in Position and Velocity Components	22

FIGURES

Figure		Page
1	Local RSS position uncertainty in earth parking orbit	23
2	Local RSS velocity uncertainty in earth parking orbit	24
3	Local RSS position uncertainties in a translunar trajectory	25
4	Local RSS velocity uncertainties in translunar trajectory	26
5	Local RSS position uncertainties in lunar orbit	27
6	Local RSS velocity uncertainties in lunar orbit	29
7	Local RSS position uncertainties in a transearth trajectory	31
8	Local RSS velocity uncertainties in a transearth trajectory	33

PRELIMINARY MSFN ERROR ANALYSIS

FOR AS-504A

By Paul H. Mitchell

SUMMARY

A theoretical error analysis of simulated observations by the Manned Space Flight Network (MSFN) was performed to ascertain the expected accuracies of the real-time orbit determination solutions at particular times during the AS-504A mission. The expected accuracies are presented at times immediately prior to all maneuvers except attitude control maneuvers and at other times of interest during the translunar, lunar parking orbit, and transearth phases.

The predicted accuracies (3-σ) at times of particular interest are: 3.1 n. mi. in position and 21.3 fps in velocity at translunar injection, 5.9 n. mi. in position and 27.6 fps in velocity at lunar orbit insertion, 1.5 n. mi. in position and 10.5 fps in velocity at powered descent to the lunar surface, 0.9 n. mi. in position and 6.2 fps in velocity at LM-CSM intercept, 0.6 n. mi. in position and 3.9 fps in velocity at transearth injection, and 0.4 n. mi. in position and 7.5 fps in velocity at reentry.

INTRODUCTION

The purpose of this internal note is to present the accuracies that can be expected for real-time orbit determination during the AS-504A mission (ref. 1) The accuracies that are presented were computed by a linear error analysis program that simulates a weighted least squares filtering technique.

The simulated observations were assumed to be obtained from various MSFN tracking stations. In numerous cases throughout the mission several tracking stations simultaneously viewed the vehicle.

When this occurred either one or three of the tracking stations, depending on the phase of the mission, was chosen to track the vehicle. The criteria employed to select the tracking station was based on the results of previous analyses which have shown that through a judicious choice of stations a certain geometric advantage can be gained that will improve orbital accuracies. However, along with the geometric considerations, it was necessary to consider the length of the view period of the available stations in order to prevent switching stations during or close to critical maneuvers.

Procedures for the selection of stations during the earth orbit phase were well established through past experience and will not be discussed here. During the translunar and transearth phases when only one station at a time was required to track the vehicle, a geometric advantage was gained by frequent switching (every 3 to 5 hours) of tracking assignments among the available stations. In operations in the vicinity of the moon, when three stations were required to track the vehicle simultaneously, a geometric advantage was gained by selecting stations that have maximum north-south and east-west separation.

The simulated tracking data were assumed to be affected by noise, biases, and station location uncertainties. Also, an uncertainty in the gravitational constant of the reference body (earth or moon) was considered. In the earth parking orbit phase, an uncertainty in the acceleration due to drag and venting was considered.

For all of the analysis it was assumed that the real-time orbit determination scheme solved for three components of position, three components of velocity, and, when three-way Doppler measurements were taken, the bias on the three-way Doppler data.

Acknowledgments are made to Samuel O. Mayfield and Larry Bonin who contributed to this document.

SYMBOLS

ANT	Antigua
ASC	Ascension Island
BDA	Bermuda Island
CDH	constant delta height (coelliptic) maneuver
CNB	Canberra

CNV	Cape Kennedy, Florida
CRO	Carnarvon, Australia
CSI	coelliptic sequence initiation
CSM	command and service modules
CYI	Grand Canary Island
EGL	Eglin Air Force Base, Florida
EOI	earth orbit insertion
EPO	earth parking orbit
ESOI	earth's sphere of influence
GBI	Grand Bahama Island
GST	Goldstone, California
GUA	Guam
GYM	Guaymas, Mexico
G&N	guidance and navigation
HAW	Kauai, Hawaii
LM	lunar module
LOI	lunar orbit insertion
LPO	lunar parking orbit
LSOI	lunar sphere of influence
MAD	Madrid, Spain
MCC	midcourse correction
MSFN	Manned Space Flight Network

ODP	orbit-determination program
RSS	root sum squared
RTCC	Real-Time Computer Complex
S-IVB	Saturn IV booster
TE	transearth
TEI	transearth injection
TEX	Corpus Christi, Texas
TL	translunar
TLI	translunar injection
TPI	terminal phase initiation
T&D	transposition and docking
USB	unified S-band

ERROR MODEL

The error model assumptions made in this analysis are presented in tables I and II and agree with those in reference 2. The uncertainty in the acceleration due to drag results from assuming a 10 percent uncertainty in the density of the 1962 Standard Atmosphere. The uncertainty in the acceleration due to venting results from assuming a 1.0-lb uncertainty in the force exerted by venting.

The execution errors for TLI, LOI, and TEI burns were determined by propagating the covariance matrix through the burn. Propagation of the covariance matrix, which was computed from the MSFN tracking data prior to the burn, was done with a computer program which considers accelerometer biases and scale factors, platform misalignment and drift, specific impulse of engine, mass, mass flow, and tail-off errors.

MSFN DESCRIPTION FOR AS-504A

The tracking stations and their equipment used in this analysis are listed in table I. The measurements made by the C-band radars were range, azimuth angle, and elevation angle. These radars were used only during the earth parking orbit phase.

Two types of USB-stations will be available for AS-504A, those having 30- and 85-ft antennas. Two basic modes of operation are available, the two-way and three-way modes. In the two-way mode, one station both transmits and receives the signal and is designated a primary station. In the three-way mode, only the primary station transmits the signal, and the secondary station receives the signal. Three-way Doppler may be obtained by more than one secondary station at the same time the primary station is receiving two-way Doppler (ref.2).

In this analysis, when three-way Doppler data were obtained, the primary station was always a station having an 85-ft antenna. In addition to Doppler data, range and x, y angle data can be obtained from the USB-stations.

DESCRIPTION OF ANALYSIS AND DATA UTILIZATION

The accuracy of real-time orbit determination solutions is presented for particular times of interest during the AS-504A mission. However, it is pointed out that the results are theoretical and are highly dependent on the assumed accuracies of the MSFN tracking instrumentation. For this analysis, the mission will be broken into five phases; earth parking orbit, translunar, lunar parking orbit, LM operations, and transearth.

Earth Parking Orbit Phase

The analysis in this phase consisted of the simulation of C-band tracking data, range and angles, where observations were taken every 6 seconds during radar view periods when the spacecraft was 5° above the horizon. Range-rate and angles were taken by the USB-stations at the same rate as the C-band data. The last station (Carnarvon) to view the vehicle prior to translunar injection was the command station which updated the onboard estimate of the state vector. Consequently, the command stations data were not considered in the reported solution. The covariance matrix determined from the earth orbit tracking data was propagated through the translunar burn. The propagated covariance matrix was then used as a priori knowledge for the initiation of the translunar phase.

Translunar Phase

The conditions at the initiation of transposition and docking were computed from two-way Doppler data taken by Hawaii (2-8 min) and Goldstone (8-15 min) at 6 second intervals. The two-way mode was used throughout the remainder of this phase. Two-way Doppler data were obtained at a rate of one observation per minute. In addition to the Doppler data, range measurements were made each hour from Goldstone, Madrid, Canberra, and Guam during the times these stations were tracking. No data were taken following lunar occultation. The covariance matrix at lunar deboost was based on the accumulated tracking data and propagated through the deboost burn. The propagated covariance matrix was then used as a priori knowledge at the initiation of the lunar parking orbit phase.

Lunar Parking Orbit Phase

During the first pass in front of the moon, two secondary stations (Antigua, Hawaii) tracked in the three-way mode, and Goldstone tracked in the two-way mode taking Doppler measurements at the rate of one

measurement every 6 seconds. The two-way mode was used for the remainder of this phase with Doppler data being taken at a rate of one observation per minute. This phase terminates at transearth injection.

The covariance matrix determined from the lunar parking orbit data was propagated through the transearth injection burn. The propagated covariance matrix was then used as a priori knowledge for the transearth phase.

LM Operations Phase

This phase begins at CSM-LM separation and ends at LM-CSM intercept. One primary and two secondary USB stations simultaneously tracked the LM during those periods that it was visible to the earth. Each station obtained Doppler data at the rate of one observation every 6 seconds.

The error analysis of the descent portion of the LM operations begins at CSM-LM separation and ends at the initiation of the powered-descent maneuver. The error analysis of the ascent portion begins at ascent burnout where it is assumed that there is no a priori knowledge of the position and velocity of the LM.

Each maneuver executed by the LM, except powered descent and launch from the lunar surface, was assumed to be impulsive. Also, it was assumed that there was an execution error of 1.0 fps in each component of the velocity.

It was assumed that there would be a voice update of the LM guidance computer prior to each of the maneuvers. Consequently, tracking was terminated 10 minutes prior to the maneuvers in order to allow time for the orbit-determination process and a voice update. For maneuvers that occurred behind the moon, tracking was terminated 10 minutes prior to lunar occultation.

Transearth Phase

Three USB-stations simultaneously tracked the CSM for the first 20 hours of the transearth phase. The two-way mode was utilized for the remainder of the phase. Both two-way and three-way Doppler data were obtained at a rate of one observation per minute throughout the transearth phase. In addition to the Doppler data, range measurements were taken by all primary stations at a rate of one observation per hour.

The solution computed at the end of tracking, when the vehicle was below 5° elevation and in the vicinity of Guam, was propagated to the nominal time of entry into the earth's atmosphere, which corresponds to approximately 400 000-ft altitude.

Although the errors assumed for the three-way Doppler biases were solved for, the errors assumed in the other biases and constants affecting the tracking data were not solved for during any phase of the mission.

Table III contains the tracking stations whose data were used in this analysis along with the view periods during which the stations were tracking. The occultation cycle was computed for the lunar parking orbit, and tracking was terminated during the occultation times. Approximately 72 minutes of data were accepted during each revolution of the CSM. The amount of data included in the LM tracking accuracy solutions varied for each maneuver and was based on G&N update and maneuver times.

ERROR ANALYSIS RESULTS

The results of this error analysis are plotted as a function of time from the beginning of each phase. The results consist of local RSS position and velocity uncertainties and represent 3-σ values of the uncertainty in the parameters based on MSFN tracking data.

The tracking coverage utilized in the study is plotted against the same time scale as the position and velocity accuracies. Thus, orbital accuracies are plotted as a function of tracking time and of MSFN tracking coverage.

The results of this analysis are summarized in table IV. Included in the table are the uncertainties in the components of position and velocity, respectively, at the initiation of the specified event. In addition to the components, the uncertainity in RSS position and velocity are presented where:

σ_x = the standard deviation in altitude

σ_y = the standard deviation in the downrange component of position

σ_z = the standard deviation in the out-of-plane component of position

$\sigma_{\dot{x}}$, $\sigma_{\dot{y}}$, $\sigma_{\dot{z}}$ = the standard deviation in altitude, downrange, and out-of-plane components of velocity, respectively

$\sigma_p = (\sigma_x^2 + \sigma_y^2 + \sigma_z^2)^{1/2}$ = RSS of standard deviations in position

$\sigma_v = (\sigma_{\dot{x}}^2 + \sigma_{\dot{y}}^2 + \sigma_{\dot{z}}^2)^{1/2}$ = RSS of standard deviations in velocity

The covariance matrices describing the accuracy of the RTCC orbit-determination program solutions at various times in the mission are included in the Appendix.

Table V contains the covariance matrices used as a priori knowledge at the initiation of the translunar, lunar parking orbit, and transearth phases. These covariance matrices were obtained by propagating the premaneuver covariance matrices through the TLI, LOI, and TEI burns, respectively.

In addition to these results, the reader is referred to reference 3 in which general error analysis studies for the AS-504A mission are reported.

Earth Parking Orbit Phase

The earth parking orbit resulted from a 72° launch azimuth and was terminated at TLI subsequent to the second pass over Carnarvon, Australia.

The error analysis results for this parking orbit (fig. 1 and 2) are consistent with those reported in reference 4 for the 72° launch azimuth, second Pacific injection, and positive lunar declination case. By comparing the present results at TLI to those in reference 4, it can be seen that they are among the best cases from the standpoint of lunar declination (launch date) but are among the worst cases from the standpoint of launch azimuth and injection position. The uncertainty in the position vector is dominated by the uncertainty in the downrange component (σ_y) and in velocity by the radial component ($\sigma_{\dot{x}}$). The major cause of the comparatively large uncertainty in these two components is the uncertainty in acceleration due to venting.

Translunar Phase

The results for this phase are in close agreement with those reported in reference 5 even though the declination of the moon differs by about 30° for the trajectories considered in the two studies. (References 1 and 5 present ground tracks of these trajectories.) This indicates that the orbital accuracies for the translunar phase of the Apollo mission are not strongly dependent on the date of the mission.

Figure 3 shows that the uncertainty in position tends to rise sharply during the first 10 to 12 hours after injection and to decrease rapidly during the last 3 to 4 hours prior to pericynthion arrival. Figure 4 shows that the uncertainty in velocity initially decreases and then increases just prior to pericynthion. The uncertainties in both position and velocity are mainly in the out-of-plane components (σ_z and $\sigma_{\dot{z}}$) throughout the entire translunar phase.

Lunar Operations

The analysis for the lunar operations phase considers MSFN tracking of the CSM in lunar parking orbit and of the LM in free-flight descent and ascent.

The figures for this phase consist of a plot of the uncertainties in position (fig. 5) and velocity (fig. 6)of the CSM during the times the LM is descending and ascending. That is, the CSM orbital uncertainties are not shown during the time the LM is on the lunar surface.

The LM position and velocity uncertainties for the nominal times of the descent and ascent maneuvers are also given as discrete entries on figures 5 and 6. Two entries are made for the LM tracking accuracies at each maneuver time. One of the entries represents the 3-σ uncertainty associated with a LM update vector based on MSFN tracking data taken 10 minutes prior to the maneuver or occultation time and propagated to the nominal time of the maneuver. The second entry is also referenced to the nominal time of the maneuver but includes MSFN tracking data up to the maneuver or occultation time.

It is pointed out that a judicious use of 3-way Doppler data would improve the CSM orbital accuracies, especially in the out-of-plane components. This is indicated by the solutions at terminal phase initiation where the LM orbit (based on 3-way data) is known better than the CSM orbit (based on 2-way data).

The uncertainties in position and velocity are dominated by the uncertainties in the out-of-plane components. That is, the uncertainties in the down-range and radial components are, in general, less than 10 percent of the total position and velocity uncertainties. Inspection of figures 5 and 6 shows that both position and velocity uncertainty plots roughly resemble a sinusoidol curve. It seems that the position is best known at the times when the vehicle's direction of motion is approximately perpendicular to the line of sight to the earth and is least known when the direction of motion is approximately parallel to the line of sight. While this seems to be true of position, the converse appears to hold for the uncertainty in velocity.

Transearth Phase

Figures 7 and 8 contain the plots of position and velocity uncertainties versus tracking time from transearth injection.

The characteristics of the position and velocity uncertainities for the transearth and translunar phases are similar in that $\sigma_{position}$ approaches a minimum near the dominating body of attraction, earth or moon, and $\sigma_{velocity}$ approaches a maximum near the attracting body.

CONCLUSIONS

1. The best orbit determination accuracy noted in the earth parking orbit occurs subsequent to the second pass over Bermuda at which time the 3-σ uncertainties in position and velocity are 0.3 n. mi. and 2.2 fps, respectively.

2. Assuming the last tracking station to view the vehicle prior to TLI (Carnarvon) is used purely as a command station the 3-σ uncertainties in position and velocity at TLI are 3.1 n. mi. and 21.3 fps, compared to 1.5 n. mi. and 11.0 fps, respectively, if the Carnarvon data are included in the error analysis solution.

3. The 3-σ uncertainties in position and velocity lie between the bounds 12 ± 2.5 n. mi. and 0.5 ± 0.25 fps, respectively, during most of the translunar phase.

4. The 3-σ uncertainties in position and velocity at the nominal time of pericynthion, computed 25 minutes prior to perciynthion arrival, are about 6.0 n. mi. and 27.5 fps of which about 2.0 n. mi. and 7 fps are in plane and the remainder is out of plane.

5. The 3-σ uncertainties in position and velocity of the CSM in lunar parking orbit levels off to less than 0.5 n. mi. and 2 fps (0.05 n. mi. and 0.2 fps in plane) as lower bounds, and 2.0 n. mi. and 5.0 fps (0.1 n. mi. and 1.0 fps in plane) as upper bounds. These bounds are approached at approximately 90° intervals, and the uncertainty in velocity approaches a minimum as the uncertainty in position approaches a maximum and vice versa.

6. At the nominal time of TEI, the CSM position and velocity can be known to within an accuracy of 1.0 n. mi. and 4 fps (3-σ).

7. The LM state vectors, computed 10 minutes prior to each maneuver, can be determined from MSFN tracking data to within a 3-σ accuracy of 2.0 n. mi. and 10.0 fps (1.0 n. mi. and 5.0 fps in plane) at the times of Hohmann transfer, powered descent, CSI, TPI, MCC, and intercept maneuvers.

8. The CDH maneuver occurs at a time when the LM is occulted by the moon, and the LM state vectors can be determined at this time to a 3-σ accuracy of about 5.0 n. mi. in position and 26.4 fps in velocity.

9. The position and velocity of the CSM in the return to earth phase are poorly determined from MSFN tracking data while it is in the LSOI. However, prior to leaving the LSOI the uncertainties in both position and velocity begin to improve considerably.

10. The 3-σ uncertainties in position and velocity at the nominal time of reentry into the earth's atmosphere are less than 1.0 n. mi. and 8.0 fps (about 0.4 n. mi. and 2.0 fps in plane), respectively.

TABLE I. - TOPOCENTRIC STATION
LOCATION UNCERTAINTIES (1σ)

Station	Type of radar	Altitude, ft	North-South component, ft	East-West component, ft
ANT	FPQ-6,30'USBS	137.8	116.4	111.6
ASC	TPQ-18,30'USBS	105.0	351.7	344.9
BDA	TPQ-6,30'USBS	141.1	120.1	121.6
CNB	85'USBS	216.5	182.3	192.5
CNV	FPS-16,30'USBS	131.2	107.1	101.4
CRO	FPQ-6,30'USBS	216.5	202.6	192.6
CYI	MPS-26	105.0	458.3	466.3
EGL	FPS-16	131.2	105.1	101.4
GBI	TPQ-18	134.5	108.9	101.4
GST	85'USBS	131.2	99.4	111.5
GUA	30'USBS	105.0	651.0	649.2
GYM	30'USBS	134.5	107.6	101.4
HAW	FPS-16,30'USBS	141.1	150.5	142.0
MAD	85'USBS	141.1	92.8	101.3
PAT	FPS-16	131.2	107.3	101.4
TEX	30'USBS	131.2	97.0	101.4

TABLE II. - DATA CHARACTERISTICS (1σ)[a]

System	Angle, m. rad.		Range, ft		Range rate, fps	
	Noise	Bias	Noise	Bias	Noise[b]	Bias
MPS-26	1.0	2.0	60	120	--	--
FPQ- 6	0.15	0.3	20	40	--	--
TPQ-18	0.2	0.4	30	60	--	--
FPS-16	0.2	0.4	30	60	--	--
USBS 30'	0.8	1.6	30	60	[c]0.12 [d]0.22	[c]0.03 [d]0.2
USBS 85'	0.8	1.6	30	60	[c]0.12	[d]0.03

[a]Uncertainties:

1-σ gravitational uncertainty of earth, $\sigma_{u_e} = 1.06 \times 10^{11} ft^3/sec^2$

1-σ gravitational uncertainty of moon, $\sigma_{u_m} = 7.1 \times 10^9 ft^3/sec^2$

1-σ drag acceleration uncertainty, $\sigma_{a_d} = 1.465 \times 10^{-6}$ ft/sec^2

where a_d is the acceleration due to drag.

1-σ venting acceleration uncertainty, $\sigma_{a_v} = 1.143 \times 10^{-4}$ ft/sec^2

where a_v is the acceleration due to venting.

[b]Based on 1-second sampling

[c]Two-way doppler, $\sigma(\dot{r}_1)$

[d]Three-way doppler, $\sigma(\dot{r}_1+\dot{r}_2)$

TABLE III.- TRACKING STATIONS VIEW PERIODS

Station	Acquisition g.e.t., day:hr:min:sec	Termination g.e.t., day:hr:min:sec	Event
BDA	0:00:11:14	0:00:11:31	EOI
CYI	0:00:17:49	0:00:22:19	
CRO	0:00:53:49	0:00:56:49	
CNB	0:01:01:25	0:01:03:44	
WHS	0:01:32:37	0:01:37:07	
CNV	0:01:36:31	0:01:40:55	
CRO	0:02:26:49	0:02:30:49	
HAW	0:02:47:53	0:02:53:28	TLI
GST	0:02:53:28	0:04:45:11	T&D
MAD	0:04:45:11	0:06:05:11	TL MCC
GST	0:06:05:11	0:08:45:11	TL Coast
GUA	0:08:45:11	0:11:45:11	
CNB	0:11:45:11	0:13:45:11	
HAW	0:13:45:11	0:16:45:11	
CNB	0:16:45:11	0:18:45:11	
MAD	0:18:45:11	0:22:45:11	
ASC	0:22:45:11	1:01:45:11	
ANT	1:01:45:11	1:04:45:11	

TABLE III.- TRACKING STATIONS VIEW PERIODS - Continued

Station	Acquisition g.e.t., day:hr:min:sec	Termination g.e.t., day:hr:min:sec	Event
GST	1:04:45:11	1:08:45:11	
HAW	1:08:45:11	1:11:45:11	
CNB	1:11:45:11	1:16:45:11	
GUA	1:16:45:11	1:20:05:11	
MAD	1:20:05:11	1:23:45:11	
ASC	1:23:45:11	2:02:45:11	
ANT	2:02:45:11	2:05:45:11	
GST	2:05:45:11	2:09:45:11	
HAW	2:09:45:11	2:12:45:11	
CNB	2:12:45:11	2:17:45:11	
GUA	2:17:45:11	2:20:45:11	
MAD	2:20:45:11	3:00:45:11	TL MCC (LSOI)
ASC	3:00:45:11	3:02:45:11	
MAD	3:02:45:11	3:04:25:11	
MAD	3:05:25:45	3:06:35:45	LOI
ASC	3:05:25:45	3:06:35:45	
BDA	3:05:25:45	3:06:35:45	
GST	3:06:35:45	3:12:22:45	

TABLE III.- TRACKING STATIONS VIEW PERIODS - Continued

Station	Acquisition g.e.t., day:hr:min:sec	Termination g.e.t., day:hr:min:sec	Event
CNB	3:12:22:45	3:20:00:45	
MAD	3:20:00:45	4:12:06:45	
GST	4:12:06:45	4:15:10:45	
CNB	4:15:10:45	4:19:33:45	
MAD	4:19:33:45	4:23:44:45	TEI
CNB	3:12:22:45	3:12:40:45	Hohmann transfer
GUA	3:12:22:45	3:12:40:45	
CRO	3:12:22:45	3:12:40:45	
CNB	3:13:32:18	3:13:51:18	Powered descent
GUA	3:13:32:18	3:13:51:18	
CRO	3:13:32:18	3:13:51:18	
CNB	4:14:34:35	4:15:02:59	CSI
GUA	4:14:34:35	4:15:02:59	
CRO	4:14:34:35	4:15:02:59	
CNB	4:15:03:06	4:15:12:00	CDH
GUA	4:15:03:00	4:15:12:00	
CRO	4:15:03:00	4:15:12:00	

TABLE III.- TRACKING STATIONS VIEW PERIODS - Continued

Station	Acquisition g.e.t., day:hr:min:sec	Termination g.e.t., day:hr:min:sec	Event
CNB	4:16:01:48	4:16:23:18	TPI
GUA	4:16:01:48	4:16:23:18	
CRO	4:16:01:48	4:16:23:18	
CNB	4:16:23:18	4:16:56:18	MCC
GUA	4:16:23:18	4:16:56:18	
CRO	4:16:23:18	4:16:56:18	
CNB	4:16:56:18	4:17:11:18	Intercept (No data taken)
MAD	4:23:50:06	5:07:30:06	TEI
BDA	4:23:50:06	5:04:30:06	
ASC	4:23:50:06	5:07:30:06	
ANT	5:04:30:06	5:12:30:06	
GST	5:07:30:06	5:15:30:06	
HAW	5:07:30:06	5:15:30:06	
GUA	5:12:30:06	5:19:30:06	
CRO	5:15:30:06	5:19:30:06	
CNB	5:15:30:06	5:20:30:06	MCC
CRO	5:20:30:06	5:23:30:06	

TABLE III.- TRACKING STATIONS VIEW PERIODS - Continued

Station	Acquisition g.e.t., day:hr:min:sec	Termination g.e.t., day:hr:min:sec	Event
MAD	5:23:30:06	6:03:30:06	
ASC	6:03:30:06	6:06:30:06	
ANT	6:06:30:06	6:09:30:06	
GST	6:09:30:06	6:13:30:06	
GUA	6:13:30:06	6:16:30:06	
CNB	6:16:30:06	6:19:30:06	
CRO	6:19:30:06	6:22:30:06	
MAD	6:22:30:06	7:02:30:06	MCC
ASC	7:02:30:06	7:07:30:06	
ANT	7:05:30:06	7:09:30:06	
GST	7:09:30:06	7:14:30:06	
GUA	7:14:30:06	7:17:30:06	
CNB	7:17:30:06	7:20:30:06	
CRO	7:20:30:06	7:23:30:06	
MAD	7:23:30:06	8:03:30:06	
ASC	8:03:30:06	8:07:30:06	

TABLE III.- TRACKING STATIONS VIEW PERIODS - Concluded

Station	Acquisition g.e.t., day:hr:min:sec	Termination g.e.t., day:hr:min:sec	Event
MAD	8:07:30:06	8:09:30:06	
ANT	8:09:30:06	8:13:30:06	
GST	8:13:30:06	8:17:30:06	
CNB	8:17:30:06	8:20:30:06	
GUA	8:20:30:06	8:22:30:06	
MAD	8:22:30:06	9:01:50:06	
GUA	9:01:50:06	9:02:30:06	

TABLE IV.- SUMMARY OF LOCAL SPACECRAFT NAVIGATIONAL ACCURACIES (3σ) FOR AS-504A

(a) RSS position and velocity uncertainties

Event	Vehicle	$3\text{-}\sigma_p$, n. mi.	$3\text{-}\sigma_v$, fps	g.e.t., day:hr:min:sec:	Reference body
TLI	CSM/LM/S-IVB	3.09	21.33	0:02:39:43	Earth
T & D	CSM/LM/S-IVB	.78	6.69	0:03:00:11	Earth
S-IVB separation + 35 minutes	CSM/LM	8.46	4.59	0:05:00:12	Earth
TL MCC - I	CSM/LM	11.13	3.93	0:05:45:11	Earth
TL MCC - II	CSM/LM	14.46	.18	2:20:45:22	Moon
LOI	CSM/LM	5.88	27.60	3:04:54:22	Moon
CSM/LM separation	CSM/LM	0.82	4.85	3:12:22:35	Moon
Hohmann transfer	CSM	0.92	2.71	3:12:52:40	Moon
	LM	0.92	2.71		
Powered descent	CSM	.30	4.95	3:13:51:10	Moon
	LM	1.50	10.51		
Plane change	CSM	.54	2.19	4:11:51:32	Moon
LM Launch	CSM	0.49	5.37	4:14:27:16	Moon
CSI	CSM	1.63	2.22	4:15:01:21	Moon
	LM	1.12	6.30		
CDH	CSM	1.47	5.28	4:15:52:05	Moon
	LM	1.21	6.78		
TPI	CSM	1.17	4.83	4:16:13:58	Moon
	LM	0.45	1.86		
MCC	CSM	.69	1.11	4:16:46:58	Moon
	LM	.48	1.35		
Intercept	LM	.84	6:15	4:17:01:37	Moon
Rendezvous	CSM/LM	1.30	4.47	4:17:12:14	Moon
TEI	CSM	.63	3.78	4:23:30:06	Moon
TE MCC - I	CSM	24.12	1.80	5:19:30:06	Earth
TE MCC - II	CSM	20.94	.57	7:01:30:06	Earth
Reentry	CM	.42	7.44	9:02:34:12	Earth

TABLE IV.- SUMMARY OF LOCAL SPACECRAFT NAVIGATIONAL ACCURACIES (3σ) FOR AS-504A

(b) Uncertainties in position and velocity components

Event	Vehicle	$3\sigma_x$, n. mi.	$3\sigma_y$, n. mi.	$3\sigma_z$, n. mi.	$3\sigma_{\dot{x}}$, fps	$3\sigma_{\dot{y}}$, fps	$3\sigma_{\dot{z}}$, fps	g.e.t. day:hr:min:sec:	Reference body
TLI	CSM/LM/S-IVB	.63	3.03	.21	21.27	1.47	.42	0:02:39:43	Earth
T & D	CSM/LM/S-IVB	.21	.15	.75	1.41	.81	6.48	0:03:00:11	Earth
S-IVB separation + 35 minutes	CSM/LM	.18	.93	8.25	.27	.69	4.53	0:05:00:12	Earth
TL MCC - I	CSM/LM	.27	1.68	9.81	.33	.78	3.81	0:05:45:11	Earth
TL MCC - II	CSM/LM	6.42	4.65	12.09	.09	.06	.15	2:20:45:22	Moon
LOI	CSM/LM	.03	1.62	5.52	6.54	2.49	27.70	3:04:54:22	Moon
CSM/LM separation	CSM/LM	0.04	0.02	0.81	0.36	.21	4.83	3:12:22:35	Moon
Hohmann transfer	CSM	0.22	0.12	0.88	1.95	0.91	1.68	3:12:52:40	Moon
	LM	0.22	0.12	0.88	1.95	0.91	1.68		
Powered descent	CSM	.03	.03	.30	.12	.24	4.95	3:13:51:10	Moon
	LM	0.03	0.13	1.52	1.00	0.17	10.46		
Plane change	CSM	.03	.06	.54	.21	.27	2.16	4:11:51:32	Moon
LM launch	CSM	.03	.09	0.47	.64	.21	5.34	4:14:27:16	Moon
CSI	CSM	.06	.03	1.63	.24	.15	2.19	4:15:01:21	Moon
	LM	.09	.12	1.11	.78	.18	6.21		
CDH	CSM	.03	.03	1.45	0.87	0.21	5.21	4:15:52:05	Moon
	LM	0.41	1.08	0.33	5.52	1.89	3.45		
TPI	CSM	.03	.06	1.16	0.75	0.21	4.77	4:16:13:58	Moon
	LM	0.05	0.05	0.44	0.45	0.24	1.80		
MCC	CSM	.03	.03	.69	.24	.21	1.05	4:16:46:58	Moon
	LM	.06	.03	.48	.24	.21	1.32		
Intercept	LM	.51	.42	.54	4.71	2.49	3.06	4:17:01:37	Moon
Rendezvous	CSM/LM	.06	0.14	1.28	.75	.21	4.38	4:17:12:14	Moon
TEI	CSM	.06	0.21	0.62	.33	.15	3.78	4:23:30:06	Moon
TE MCC - I	CSM	.09	11.01	21.42	.24	1.02	1.47	5:19:30:06	Earth
TE MCC - II	CSM	.69	11.76	17.31	.03	.36	.45	7:01:30:06	Earth
Reentry	CM	.12	.36	.21	1.77	.45	7.20	9:02:34:12	Earth

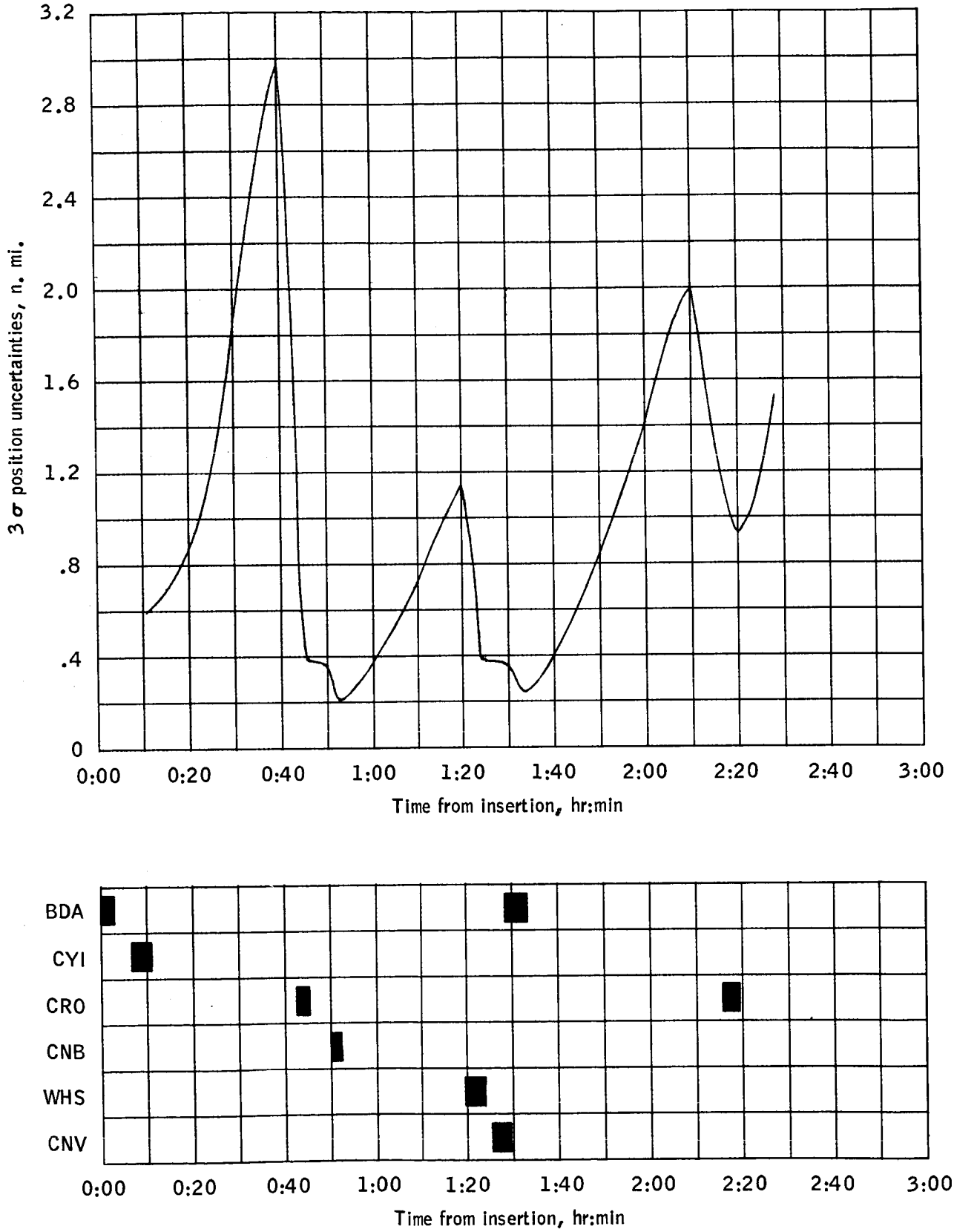

Figure 1.- Local RSS position uncertainty in earth parking orbit.

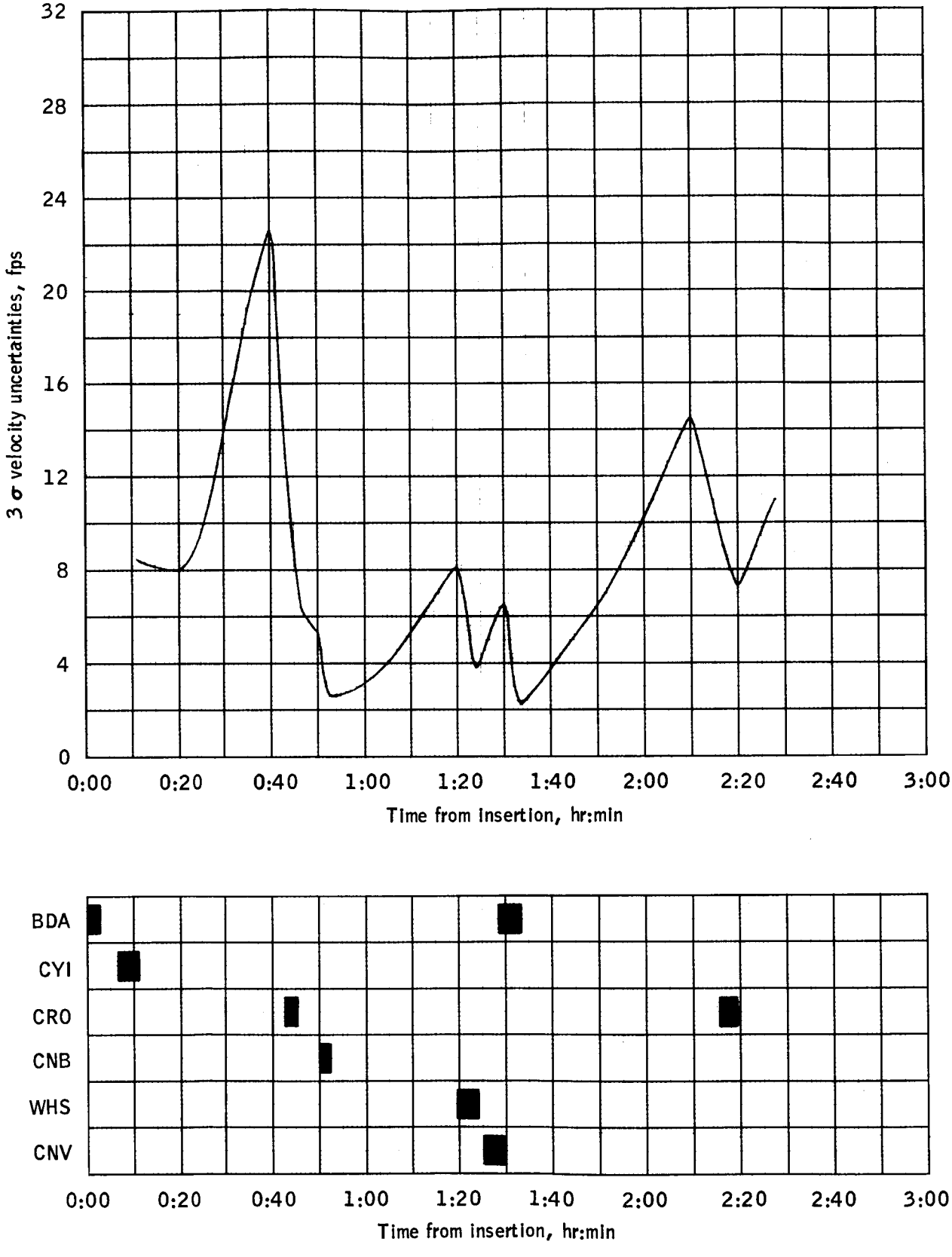

Figure 2.- Local RSS velocity uncertainty in earth parking orbit.

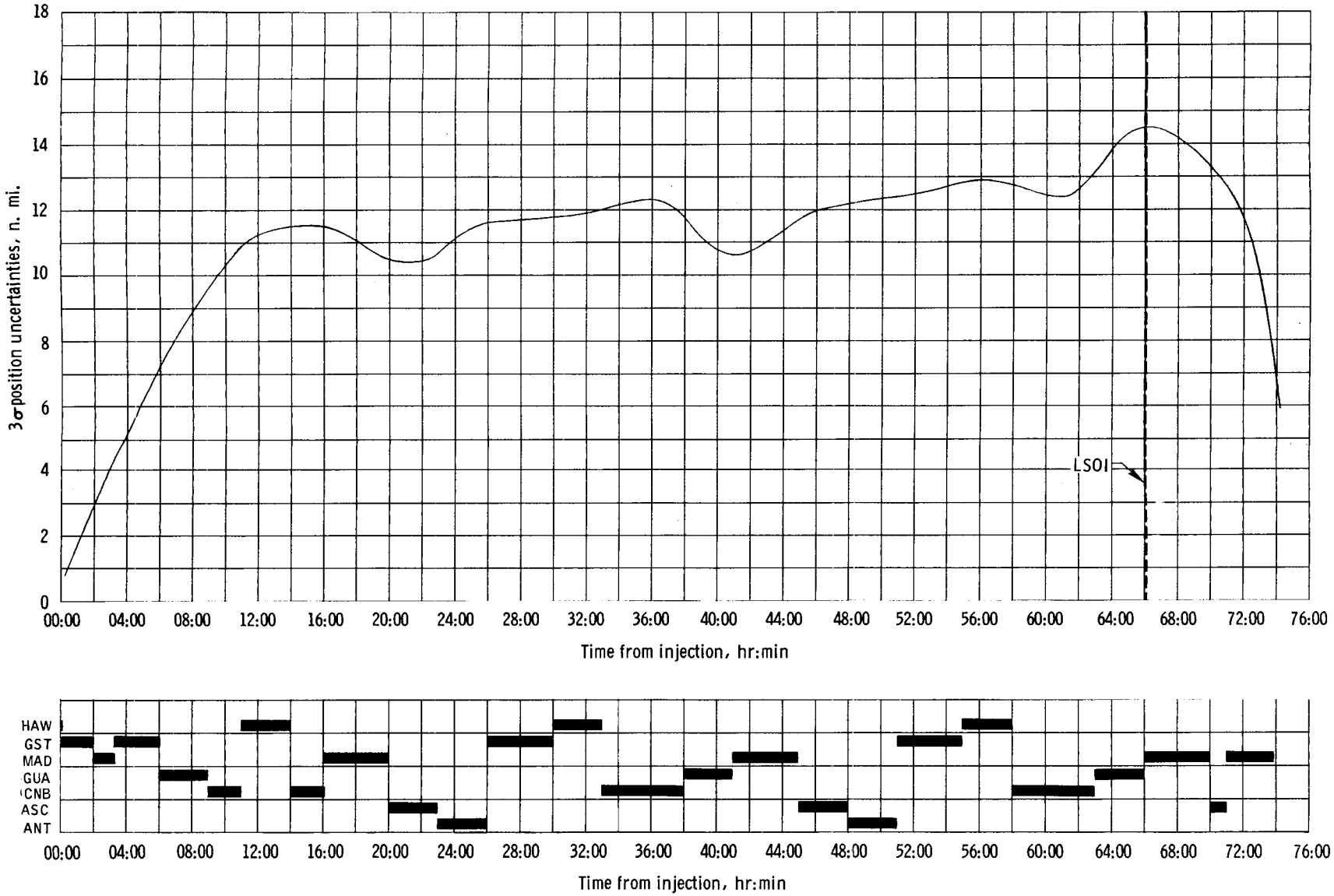

Figure 3. - Local RSS position uncertainties in a translunar trajectory.

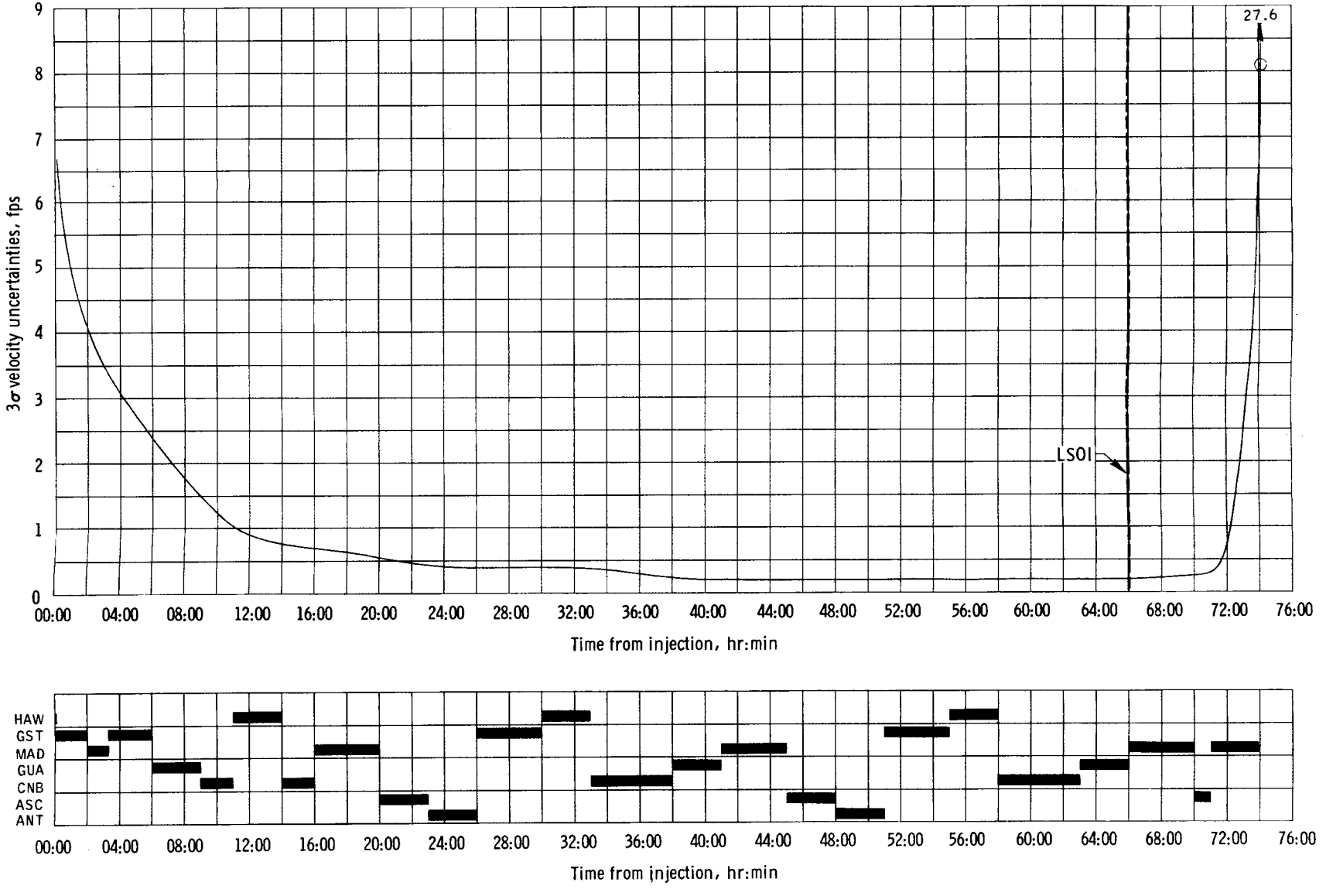

Figure 4. - Local RSS velocity uncertainties in translunar trajectory.

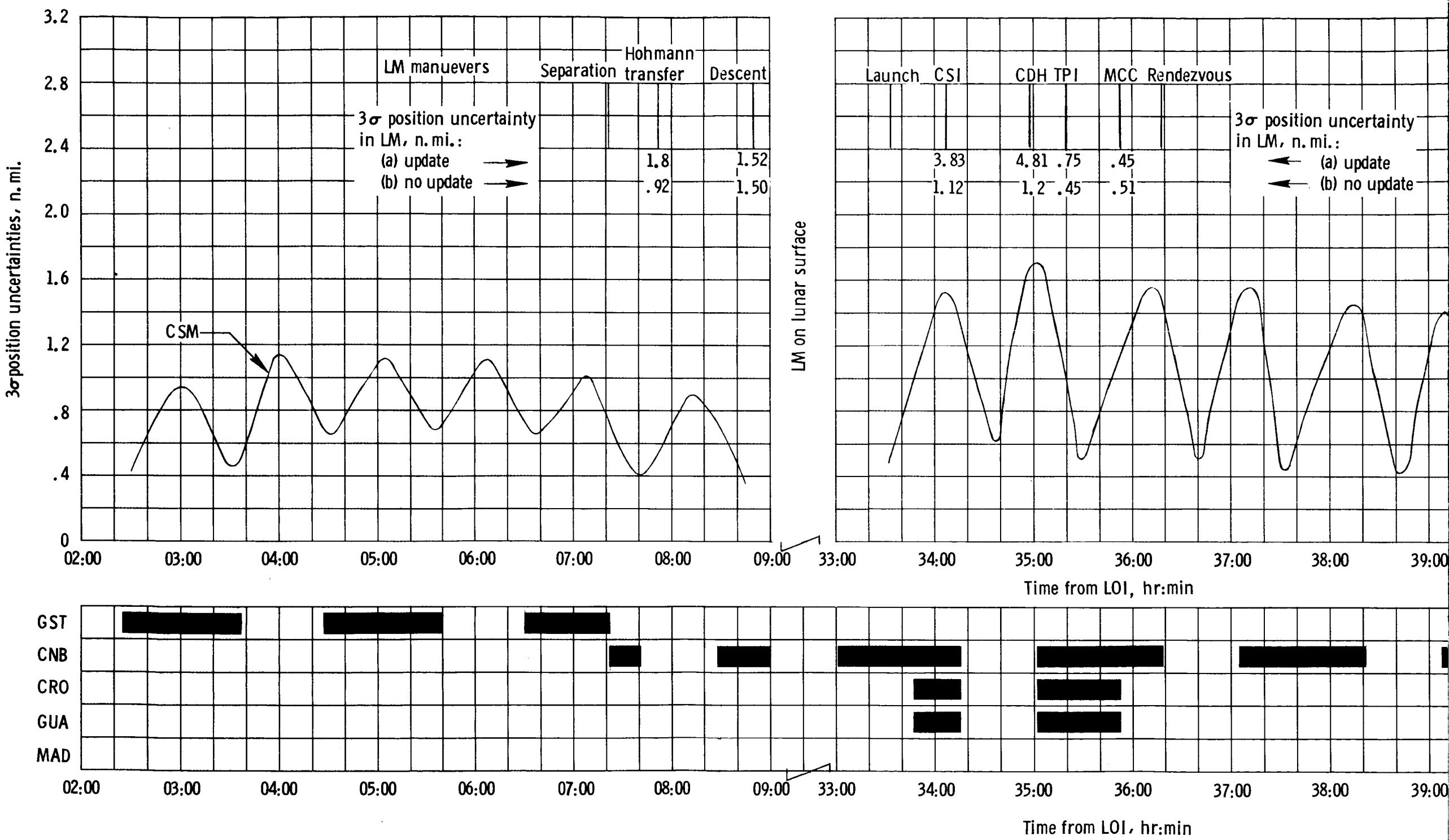

FOLD-OUT #1

Figure 5. - Local RSS position uncertainties in lunar orbit.

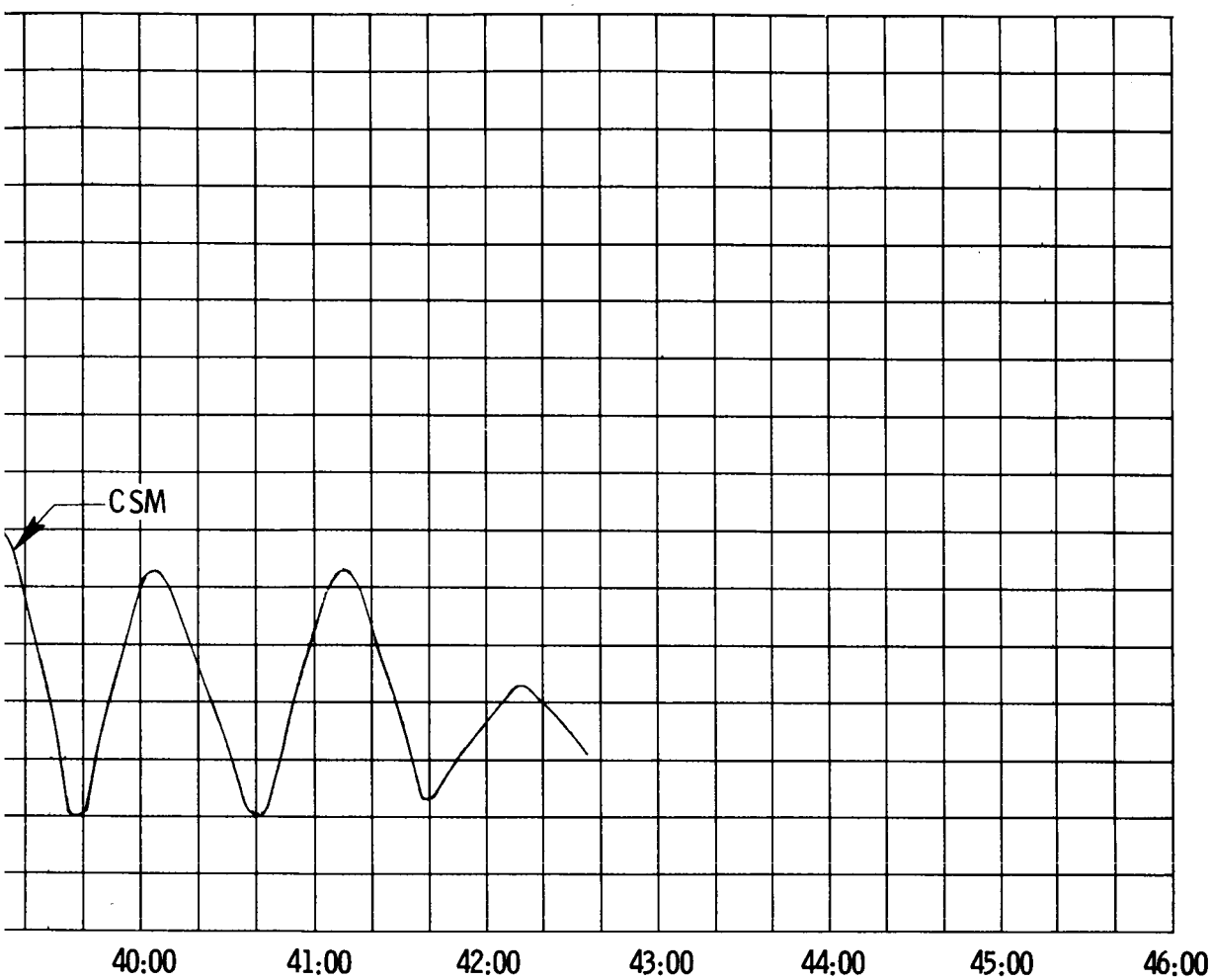
CSM
40:00
41:00
42:00
43:00
44:00
45:00
46:00

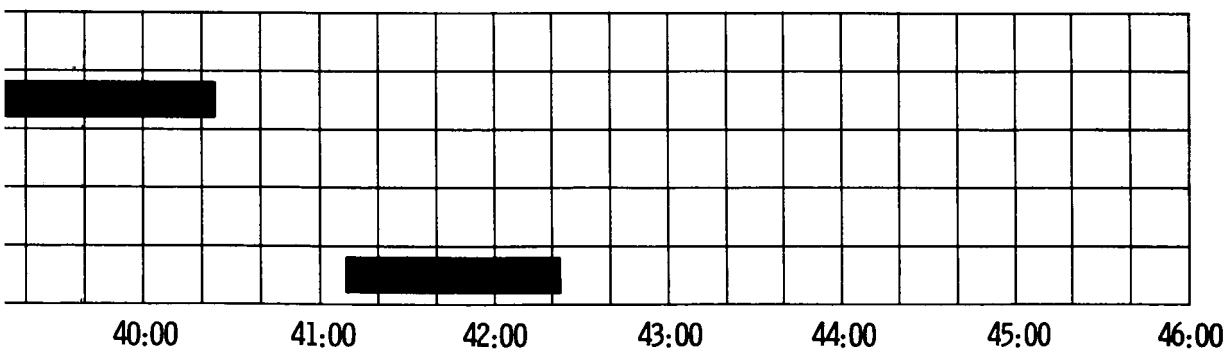
40:00
41:00
42:00
43:00
44:00
45:00
46:00

FOLD-OUT #2

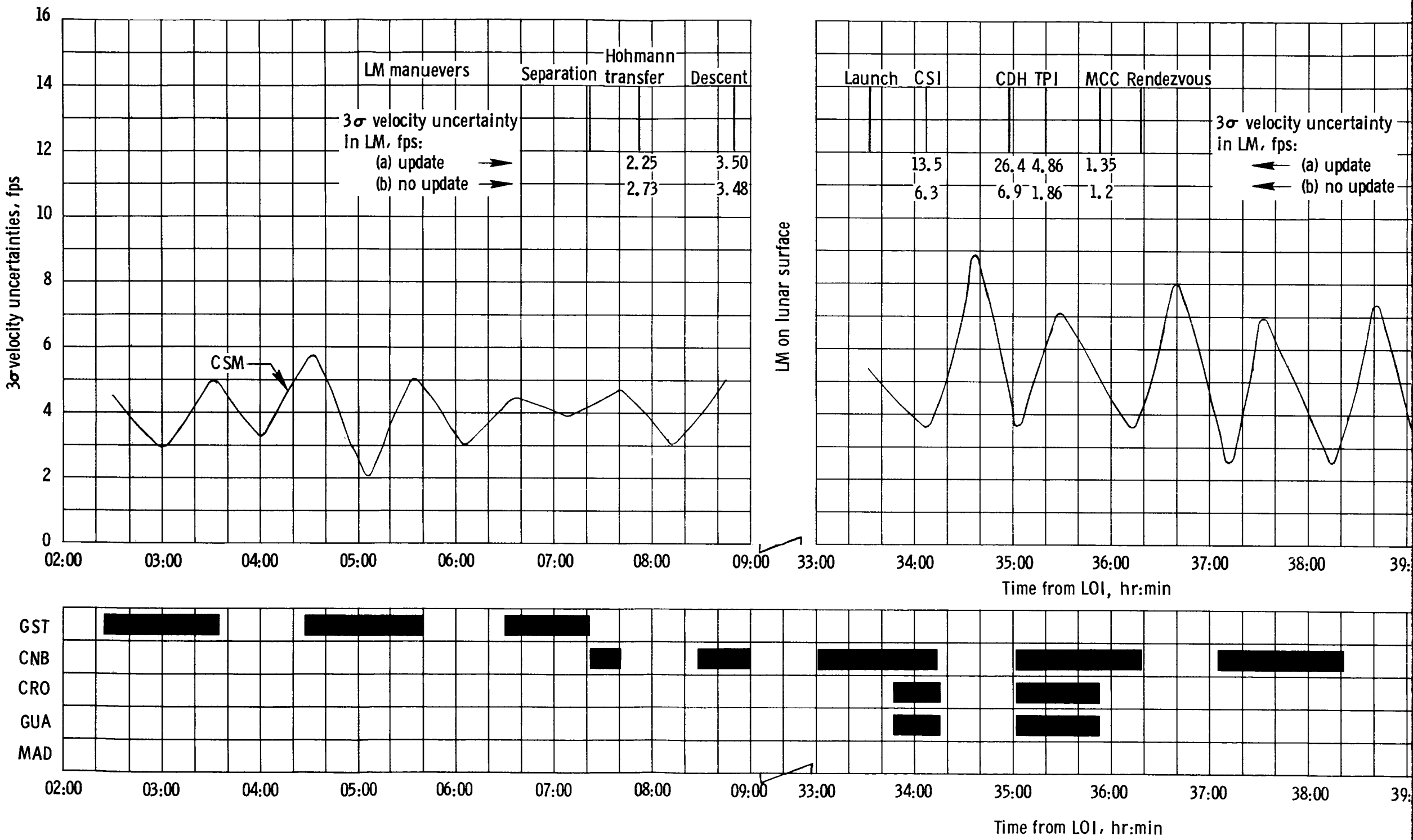

FOLD-OUT #1

Figure 6. - Local RSS velocity uncertainties in lunar orbit.

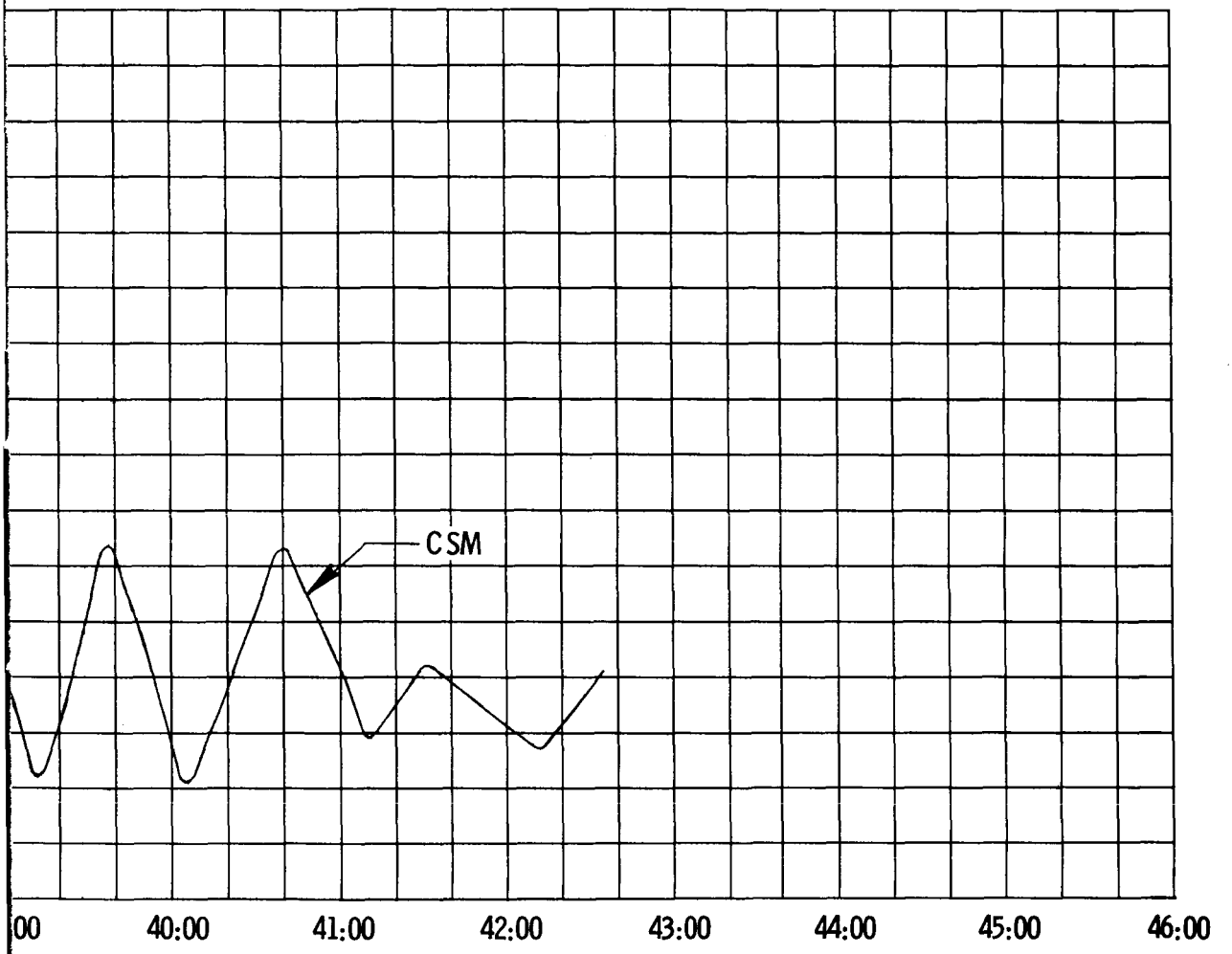
CSM
00
40:00
41:00
42:00
43:00
44:00
45:00
46:00

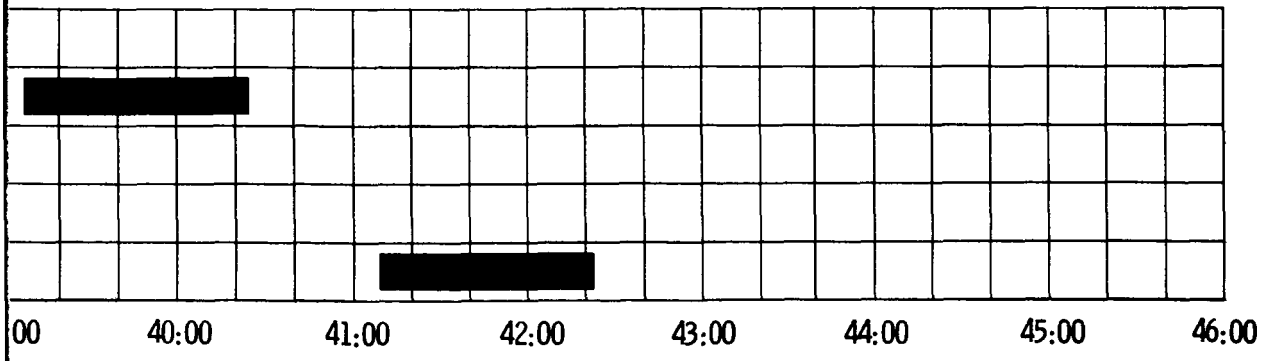
00
40:00
41:00
42:00
43:00
44:00
45:00
46:00

FOLD-OUT #2

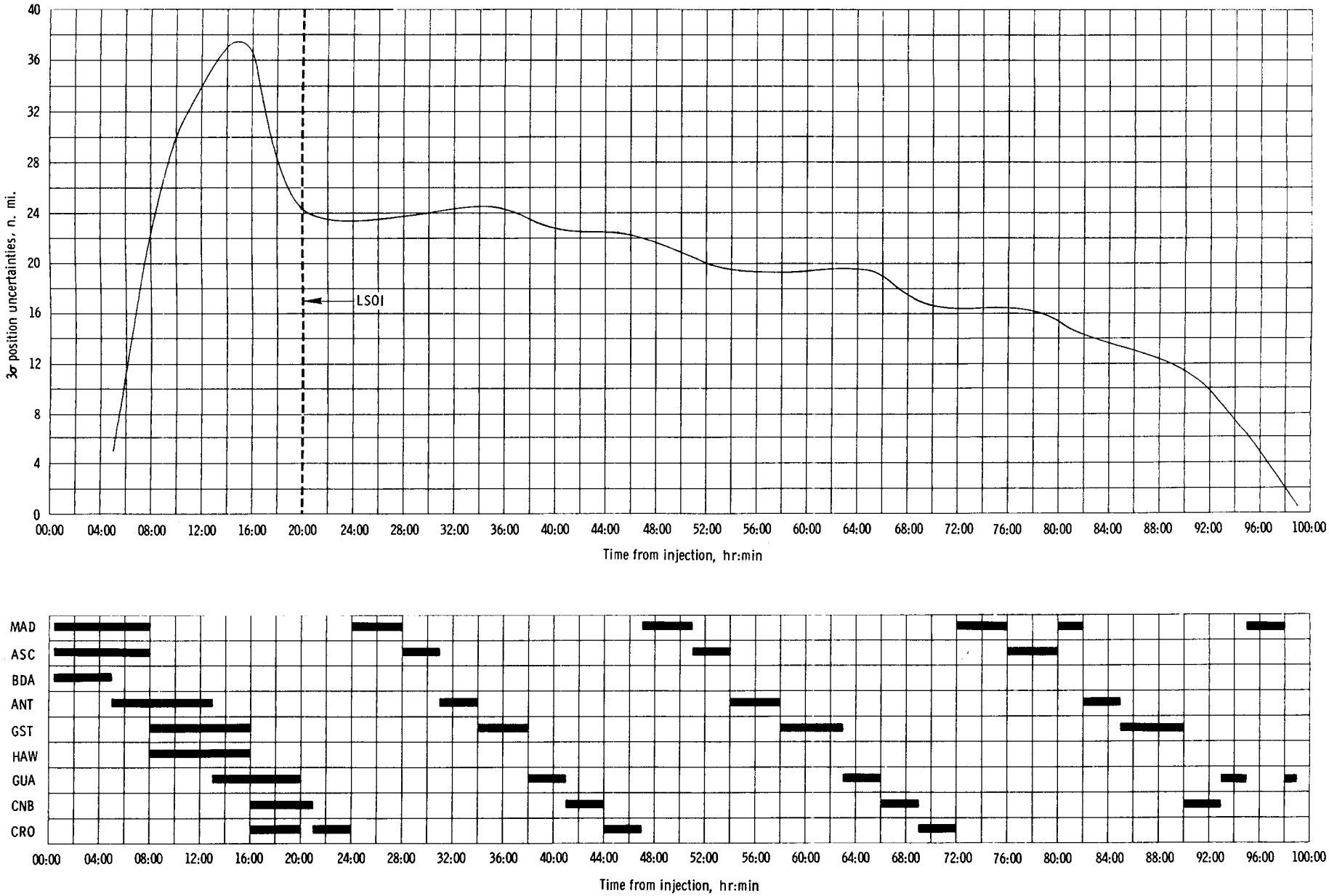

Figure 7. - Local RSS position uncertainties in a transearth trajectory.

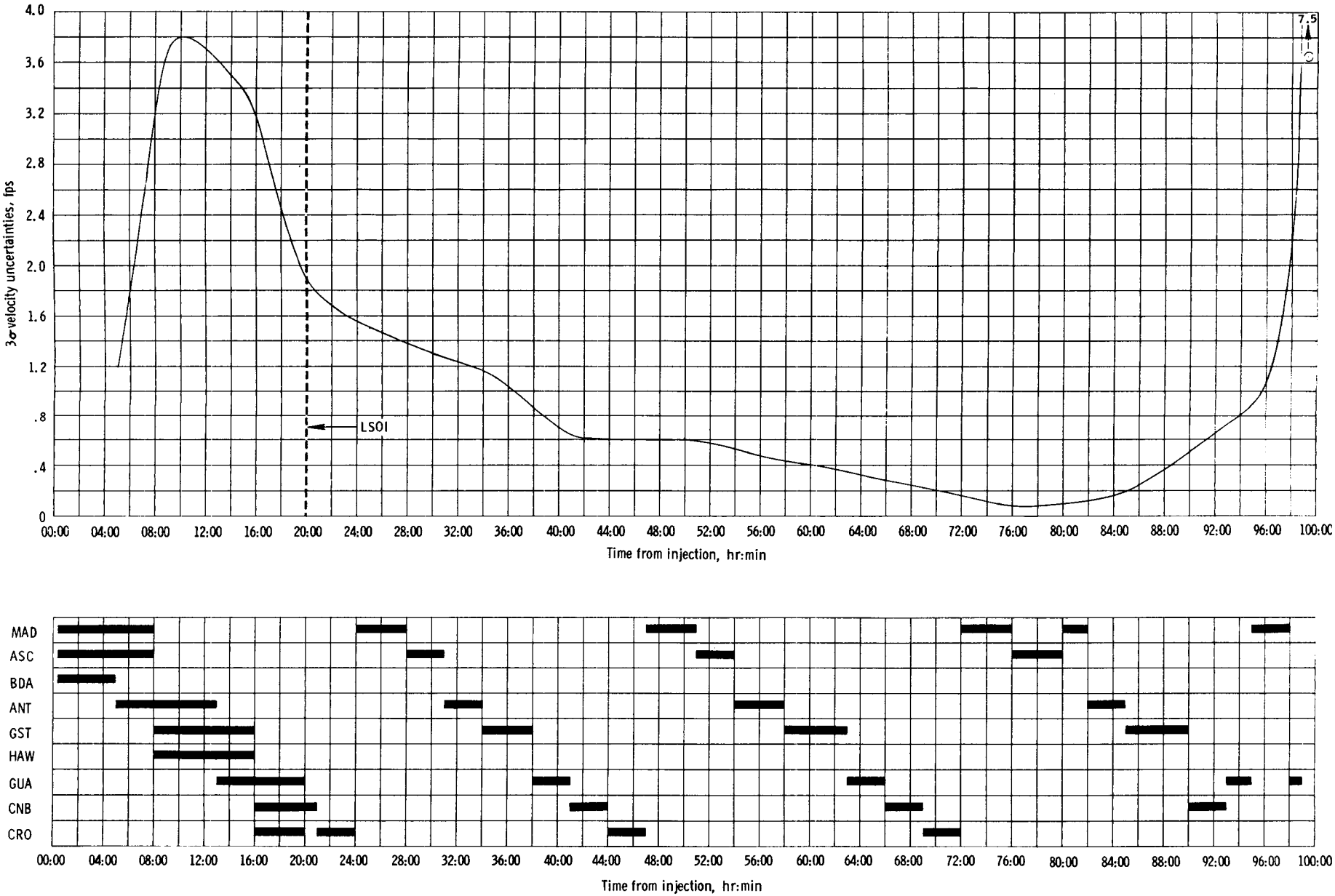

Figure 8. - Local RSS velocity uncertainties in a transearth trajectory.

APPENDIX

COVARIANCE MATRICES

APPENDIX

COVARIANCE MATRICES

TABLE A-I.- 1-σ COVARIANCE MATRICES

Format for Covariance Matrices

$$\begin{bmatrix} \sigma_{xx} & \sigma_{xy} & \sigma_{xz} & \sigma_{x\dot{x}} & \sigma_{x\dot{y}} & \sigma_{x\dot{z}} \\ & \sigma_{yy} & \sigma_{yz} & \sigma_{y\dot{x}} & \sigma_{y\dot{y}} & \sigma_{y\dot{z}} \\ & & \sigma_{zz} & \sigma_{z\dot{x}} & \sigma_{z\dot{y}} & \sigma_{z\dot{z}} \\ & & & \sigma_{\dot{x}\dot{x}} & \sigma_{\dot{x}\dot{y}} & \sigma_{\dot{x}\dot{z}} \\ & & & & \sigma_{\dot{y}\dot{y}} & \sigma_{\dot{y}\dot{z}} \\ & & & & & \sigma_{\dot{z}\dot{z}} \end{bmatrix}$$

The coordinate system for the covariance matrices is as follows:

x is in the direction of the vehicles radius vector from the reference body (earth or moon) at the time of the event.

y is in the vehicle's orbital plane about the reference body in the direction of the vehicle motion and is orthogonal to x.

z is orthogonal to both x and y such that (x,y,z)forms a righthanded, rectangular Cartesian coordinate system.

The units for position and velocity are feet and feet per second, respectively.

1. Covariance Matrix at TLI

.160544+07	-.770124+07	-.101735+06	.892079+04	-.609188+03	-.274474+02
-.770124+07	.374792+08	.517895+06	-.434255+05	.291684+04	.138807+03
-.101735+06	.517895+06	.154770+06	-.570909+03	.501786+02	.194212+02
.892079+04	-.434255+05	-.570909+03	.503305+02	-.337504+01	-.159998-00
-.609188+03	.291684+04	.501786+02	-.337504+01	.241263-00	.110535-01
-.274474+02	.138807+03	.194212+02	-.159998-00	.110535-01	.193774-01

2. Covariance Matrix at Transposition and Docking

0.167290E 06	-0.890819E 05	0.533732E 06	0.177065E 03	-0.909612E 02	0.746066E 03
-0.890819E 05	0.801574E 05	-0.275961E 06	-0.122271E 03	0.676498E 02	-0.346269E 03
0.533732E 06	-0.275961E 06	0.189600E 07	0.565400E 03	-0.302232E 03	0.268226E 04
0.177065E 03	-0.122271E 03	0.565400E 03	0.220181E-00	-0.119893E-00	0.778735E 00
-0.909612E 02	0.676498E 02	-0.302232E 03	-0.119893E-00	0.737211E-01	-0.419192E-00
0.746066E 03	-0.346269E 03	0.268226E 04	0.778735E 00	-0.419192E-00	0.402007E 01

3. Covariance Matrix at TLI + 1 hour

0.720732E 05	-0.183412E 06	0.791545E 06	0.231378E 02	-0.438801E 02	0.180904E 03
-0.183412E 06	0.822763E 06	0.220455E 06	-0.119114E 03	0.226793E 03	-0.168339E 02
0.791545E 06	0.220455E 06	0.620752E 08	-0.544907E 03	0.678226E 03	0.124866E 05
0.231378E 02	-0.119114E 03	-0.544907E 03	0.224982E-01	-0.384970E-01	-0.983311E-01
-0.438801E 02	0.226793E 03	0.678226E 03	-0.384970E-01	0.713389E-01	0.112516E-00
0.180904E 03	-0.168339E 02	0.124866E 05	-0.983311E-01	0.112516E-00	0.254319E 01

4. Covariance Matrix at TLI + 2 hours

0.116896E 06	-0.488712E 06	0.179837E 07	0.227931E 02	-0.526869E 02	0.176361E 03
-0.488712E 06	0.361916E 07	-0.644122E 07	-0.140593E 03	0.412818E 03	-0.667125E 03
0.179837E 07	-0.644122E 07	0.285778E 09	-0.319302E 03	0.327067E 03	0.253337E 05
0.227931E 02	-0.140593E 03	-0.319302E 03	0.750129E-02	-0.182007E-01	-0.238924E-01
-0.526869E 02	0.412818E 03	0.327067E 03	-0.182007E-01	0.519882E-01	0.149438E-01
0.176361E 03	-0.667125E 03	0.253337E 05	-0.238924E-01	0.149438E-01	0.225816E 01

5. Covariance Matrix at TL MCC 1

0.296899E 06	-0.151541E 07	0.850501E 07	0.545232E 02	-0.110180E 03	0.505332E 03
-0.151541E 07	0.115679E 08	-0.344069E 08	-0.351848E 03	0.877974E 03	-0.212027E 04
0.850501E 07	-0.344069E 08	0.496980E 09	0.147812E 04	-0.211474E 04	0.283241E 05
0.545232E 02	-0.351848E 03	0.147812E 04	0.119163E-01	-0.264766E-01	0.890302E-01
-0.110180E 03	0.877974E 03	-0.211474E 04	-0.264766E-01	0.679950E-01	-0.134740E-00
0.505332E 03	-0.212027E 04	0.283241E 05	0.890302E-01	-0.134740E-00	0.162275E 01

6. Covariance Matrix at TLI + 6 hours

0.111943E 07	-0.408752E 07	0.272245E 08	0.972064E 02	-0.135745E 03	0.730397E 03
-0.408752E 07	0.343536E 08	-0.105166E 09	-0.466814E 03	0.118454E 04	-0.293457E 04
0.272245E 08	-0.105166E 09	0.804795E 09	0.254650E 04	-0.348393E 04	0.214463E 05
0.972064E 02	-0.466814E 03	0.254650E 04	0.950471E-02	-0.159158E-01	0.689174E-01
-0.135745E 03	0.118454E 04	-0.348393E 04	-0.159158E-01	0.412266E-01	-0.982380E-01
0.730397E 03	-0.293457E 04	0.214463E 05	0.689174E-01	-0.982380E-01	0.575002E 00

7. Covariance Matrix at TLI + 11 hours

0.515191E 06	-0.682989E 06	0.675928E 07	0.171199E 02	-0.100280E 02	0.897151E 02
-0.682989E 06	0.683630E 08	-0.945745E 08	-0.182419E 03	0.119816E 04	-0.142524E 04
0.675928E 07	-0.945745E 08	0.422747E 09	0.465542E 03	-0.155298E 04	0.574739E 04
0.171199E 02	-0.182419E 03	0.465542E 03	0.119854E-02	-0.327654E-02	0.668852E-02
-0.100280E 02	0.119816E 04	-0.155298E 04	-0.327654E-02	0.212133E-01	-0.239926E-01
0.897151E 02	-0.142524E 04	0.574739E 04	0.668852E-02	-0.239926E-01	0.799347E-01

8. Covariance Matrix at TLI + 16 hours

0.100579E 07	-0.109157E 07	0.124667E 08	0.251121E 02	-0.113100E 02	0.107793E 03
-0.109157E 07	0.703123E 08	-0.629791E 08	-0.150172E 03	0.844744E 03	-0.702377E 03
0.124667E 08	-0.629791E 08	0.424750E 09	0.472313E 03	-0.720013E 03	0.385099E 04
0.251121E 02	-0.150172E 03	0.472313E 03	0.109620E-02	-0.188270E-02	0.449179E-02
-0.113100E 02	0.844744E 03	-0.720013E 03	-0.188270E-02	0.102678E-01	-0.835806E-02
0.107793E 03	-0.702377E 03	0.385099E 04	0.449179E-02	-0.835806E-02	0.361453E-01

9. Covariance Matrix at TLI + 21 hours

0.114790E 07	0.158563E 07	0.776394E 07	0.152017E 02	0.160348E 02	0.430117E 02
0.158563E 07	0.900471E 08	-0.611871E 09	-0.750270E 02	0.796289E 03	-0.539965E 03
0.776394E 07	-0.611871E 08	0.349670E 09	0.189816E 03	-0.490970E 03	0.233976E 04
0.152017E 02	-0.750270E 02	0.189816E 03	0.507959E-03	-0.737647E-03	0.138960E-02
0.160348E 02	0.796289E 03	-0.490970E 03	-0.737647E-03	0.713666E-02	-0.464294E-02
0.430117E 02	-0.539965E 03	0.233976E 04	0.138960E-02	-0.464294E-02	0.166133E-01

10. Covariance Matrix at TLI + 26 hours

0.185532E 07	0.504969E 07	0.105234E 08	0.199799E 02	0.362994E 02	0.441665E 02
0.504969E 07	0.139663E 09	-0.900175E 08	-0.340527E 02	0.954094E 03	-0.585275E 03
0.105234E 08	-0.900175E 08	0.409965E 09	0.215365E 03	-0.583459E 03	0.216703E 04
0.199799E 02	-0.340527E 02	0.215365E 03	0.450459E-03	-0.297438E-03	0.118536E-02
0.362994E 02	0.954094E 03	-0.583459E 03	-0.297438E-03	0.659414E-02	-0.401434E-02
0.441665E 02	-0.585275E 03	0.216703E 04	0.118536E-02	-0.401434E-02	0.122370E-01

11. Covariance Matrix at TLI + 31 hours

0.152488E 07	0.372681E 07	0.491410E 07	0.143637E 02	0.214597E 02	0.148020E 02
0.372681E 07	0.147782E 09	-0.118987E 09	-0.291018E 02	0.823209E 03	-0.608643E 03
0.491410E 07	-0.118987E 09	0.417277E 09	0.107309E 03	-0.635237E 03	0.184568E 04
0.143637E 02	-0.291018E 02	0.107309E 03	0.317800E-03	-0.236055E-03	0.568953E-03
0.214597E 02	0.823209E 03	-0.635237E 03	-0.236055E-03	0.465171E-02	-0.343020E-02
0.148020E 02	-0.608643E 03	0.184568E 04	0.568953E-03	-0.343020E-02	0.879907E-02

12. Covariance Matrix at TLI + 36 hours

0.133185E 07	0.668127E 07	-0.600852E 07	0.969065E 01	0.312880E 02	-0.275691E 02
0.668127E 07	0.164204E 09	-0.160728E 09	-0.489951E 01	0.769122E 03	-0.673265E 03
-0.600852E 07	-0.160728E 09	0.456094E 09	0.100667E 02	-0.728738E 03	0.172715E 04
0.969065E 01	-0.489951E 01	0.100667E 02	0.231850E-03	-0.100041E-03	0.149767E-03
0.312880E 02	0.769122E 03	-0.728738E 03	-0.100041E-03	0.366419E-02	-0.321194E-02
-0.275691E 02	-0.673265E 03	0.172715E 04	0.149767E-03	-0.321194E-02	0.708320E-02

13. Covariance Matrix at TLI + 41 hours

0.101923E 07	0.323006E 07	-0.345498E 07	0.888818E 01	0.127993E 02	-0.148988E 02
0.323006E 07	0.145534E 09	-0.905418E 08	-0.190819E 02	0.596228E 03	-0.369790E 03
-0.345498E 07	-0.905418E 08	0.313151E 09	0.124563E 02	-0.363998E 03	0.105130E 04
0.888818E 01	-0.190819E 02	0.124563E 02	0.239583E-03	-0.157779E-03	0.168497E-03
0.127993E 02	0.596228E 03	-0.363998E 03	-0.157779E-03	0.249740E-02	-0.162718E-02
-0.148988E 02	-0.369790E 03	0.105130E 04	0.168497E-03	-0.162718E-02	0.402524E-02

14. Covariance Matrix at TLI + 46 hours

0.139892E 07	0.871739E 06	0.425600E 07	0.117744E 02	0.354760E 01	0.576226E 01
0.871739E 06	0.160607E 09	-0.116877E 09	-0.341050E 02	0.570402E 03	-0.384225E 03
0.425600E 07	-0.116877E 09	0.425012E 09	0.548304E 02	-0.391595E 03	0.118454E 04
0.117744E 02	-0.341050E 02	0.548304E 02	0.250012E-03	-0.191672E-03	0.251419E-03
0.354760E 01	0.570402E 03	-0.391595E 03	-0.191672E-03	0.208100E-02	-0.143419E-02
0.576226E 01	-0.384225E 03	0.118454E 04	0.251419E-03	-0.143419E-02	0.377097E-02

15. Covariance Matrix at TLI + 51 hours

0.186323E 07	0.290458E 07	0.665040E 07	0.153464E 02	0.900135E 01	0.115382E 02
0.296458E 07	0.210708E 09	-0.134683E 09	-0.245077E 02	0.653661E 03	-0.366458E 03
0.665040E 07	-0.134683E 09	0.433982E 09	0.783385E 02	-0.400202E 03	0.106419E 04
0.153464E 02	-0.245077E 02	0.783385E 02	0.267116E-03	-0.149069E-03	0.290348E-03
0.900135E 01	0.653661E 03	-0.400202E 03	-0.149069E-03	0.208492E-02	-0.123142E-02
0.115382E 02	-0.366458E 03	0.106419E 04	0.290348E-03	-0.123142E-02	0.304740E-02

16. Covariance Matrix at TLI + 56 hours

0.116979E 07	0.456376E 06	0.535132E 07	0.109126E 02	0.423359E-00	0.104312E 02
0.456376E 06	0.229401E 09	-0.157310E 09	-0.375957E 02	0.631033E 03	-0.367001E 03
0.535132E 07	-0.157310E 09	0.448717E 09	0.613372E 02	-0.410273E 03	0.983534E 03
0.109126E 02	-0.375957E 02	0.613372E 02	0.228872E-03	-0.183598E-03	0.254512E-03
0.423359E-00	0.631033E 03	-0.410273E 03	-0.183598E-03	0.180041E-02	-0.110275E-02
0.104312E 02	-0.367001E 03	0.983534E 03	0.254512E-03	-0.110275E-02	0.254614E-02

17. Covariance Matrix at TLI + 61 hours

0.884322E 06	0.249909E 07	0.103984E 07	0.881947E 01	0.450683E 01	0.298806E 01
0.249909E 07	0.276826E 09	-0.190365E 09	-0.251324E 02	0.677838E 03	-0.392606E 03
0.103984E 07	-0.190365E 09	0.457803E 09	0.322910E 02	-0.436015E 03	0.907128E 03
0.881947E 01	-0.251324E 02	0.322910E 02	0.204880E-03	-0.153182E-03	0.194252E-03
0.450683E 01	0.677838E 03	-0.436015E 03	-0.153182E-03	0.174273E-02	-0.105684E-02
0.298806E 01	-0.392606E 03	0.907128E 03	0.194252E-03	-0.105684E-02	0.213861E-02

18. Covariance Matrix at TL MCC 2 (Moon-centered coordinates) (LSOI)

0.168319E 09	0.120994E 09	0.152627E 09	0.303735E 03	0.230882E 03	0.266985E 03
0.120994E 09	0.887332E 08	0.128157E 09	0.210408E 03	0.177893E 03	0.235133E 03
0.152627E 09	0.128157E 09	0.600503E 09	0.186591E 03	0.287382E 03	0.126248E 04
0.303735E 03	0.210408E 03	0.186591E 03	0.637050E-03	0.384017E-03	0.340146E-03
0.230882E 03	0.177893E 03	0.287382E 03	0.384017E-03	0.578530E-03	0.758303E-03
0.266985E 03	0.235133E 03	0.126248E 04	0.340146E-03	0.758303E-03	0.294886E-02

19. Covariance Matrix at LSOI + 5 hours.

0.293439E 08	0.163652E 08	0.481703E 08	0.302885E 03	-0.453017E 02	-0.140324E 03
0.163652E 08	0.130384E 08	0.639195E 08	0.157220E 03	-0.221651E 02	-0.183249E 03
0.481703E 08	0.639195E 08	0.614294E 09	0.395556E 03	-0.110487E 03	-0.182605E 04
0.302885E 03	0.157220E 03	0.395556E 03	0.344885E-02	-0.431395E-03	-0.106531E-02
-0.453017E 02	-0.221651E 02	-0.110487E 03	-0.431395E-03	0.216236E-03	0.503927E-03
-0.140324E 03	-0.183249E 03	-0.182605E 04	-0.106531E-02	0.503927E-03	0.569077E-02

20. Covariance Matrix at Lunar Deboost

0.559769E 07	-0.684422E 07	0.244670E 08	0.485430E 04	-0.190269E 04	-0.194311E 05
-0.684422E 07	0.109820E 08	-0.273556E 08	-0.711983E 04	0.206413E 04	0.217298E 05
0.244670E 08	-0.273556E 08	0.125630E 09	0.201474E 05	-0.872877E 04	-0.998052E 05
0.485430E 04	-0.711983E 04	0.201474E 05	0.475401E 01	-0.154044E 01	-0.160022E 02
-0.190269E 04	0.206413E 04	-0.872877E 04	-0.154044E 01	0.685089E 00	0.693169E 01
-0.194311E 05	0.217298E 05	-0.998052E 05	-0.160022E 02	0.693169E 01	0.792901E 02

21. Covariance Matrix at CSM/LM separation

.740332+04	-.144963+03	-.786158+05	.313854-00	.591844+01	.888281+02
-.144963+03	.197199+05	.181503+06	-.173564+02	.161634+01	.168778+03
-.786158+05	.181503+06	.268836+07	-.158677+03	-.538151+02	.684052+03
.313854-00	-.173564+02	-.158677+03	.154227-01	-.154381-02	-.146873-00
.591844+01	.161634+01	-.538151+02	-.154381-02	.540717-02	.865424-01
.888281+02	.168778+03	.684052+03	-.146873-00	.865424-01	.290059+01

22. CSM Covariance Matrix at Hohmann Transfer

.192917+06	-.102965+06	-.775560+06	.283484+03	-.133213+03	-.906924+02
-.102965+06	.581800+05	.403559+06	-.152241+03	.713673+02	.482956+02
-.775560+06	.403559+06	.320615+07	-.114401+04	.541136+03	.485405+03
.283484+03	-.152241+03	-.114401+04	.417838-00	-.196699-00	-.149475-00
-.133213+03	.713673+02	.541136+03	-.196699-00	.927720-01	.768468-01
-.906924+02	.482956+02	.485405+03	-.149475-00	.768468-01	.308503-00

23. CSM Covariance Matrix at Powered Descent

.115116+05	.454753+04	-.256658+05	-.188139+01	.532178+01	-.749857+02
.454753+04	.205728+04	-.176139+05	-.147660+01	.254129+01	-.310221+02
-.256658+05	-.176139+05	.143195+06	.884311+01	-.191830+02	.182951+03
-.188139+01	-.147660+01	.884311+01	.101590-02	-.840256-03	.126928-01
.532178+01	.254129+01	-.191830+02	-.840256-03	.319381-02	-.361599-01
-.749857+02	-.310221+02	.182951+03	.126928-01	-.361599-01	.493142-00

24. CSM Covariance Matrix at CSM Plane Change

0.575158E 04	-0.332926E 04	0.721716E 05	0.198938E 01	0.674533E 01	-0.511885E 02
-0.332926E 04	0.992368E 04	-0.812898E 05	-0.703229E 01	-0.479935E 01	0.234390E 02
0.721716E 05	-0.812898E 05	0.117467E 07	0.525542E 02	0.858230E 02	-0.564428E 03
0.198938E 01	-0.703229E 01	0.525542E 02	0.506659E-02	0.298139E-02	-0.133125E-01
0.674533E 01	-0.479935E 01	0.858230E 02	0.298139E-02	0.838162E-02	-0.637903E-01
-0.511885E 02	0.234390E 02	-0.564428E 03	-0.133125E-01	-0.637903E-01	0.516115E 00

25. CSM Covariance Matrix 10 Minutes Prior to LM Launch

0.508280E 04	-0.120182E 05	-0.373185E 04	0.109765E 02	0.606637E 01	-0.796123E 02
-0.120182E 05	0.299782E 05	0.190730E 05	-0.277199E 02	-0.141432E 02	0.179597E 03
-0.373185E 04	0.190730E 05	0.926045E 05	-0.198562E 02	0.178340E 01	-0.667096E 02
0.109765E 02	-0.277199E 02	-0.198562E 02	0.257080E-01	0.128458E-01	-0.161621E-00
0.606637E 01	-0.141432E 02	0.178340E 01	0.128458E-01	0.840593E-02	-0.111399E-00
-0.796123E 02	0.179597E 03	-0.667096E 02	-0.161621E-00	-0.111399E-00	0.150424E 01

26. CSM Covariance Matrix at LM Launch (time = t), Computed at t - 10 minutes

.712126+04	-.607420+04	-.628415+05	.516220+01	.610056+01	-.752025+02
-.607420+04	.434102+05	-.584367+05	-.376894+02	-.498806+01	.364089+03
-.628415+05	-.584367+05	.900188+06	.503415+02	-.553121+02	-.212378+03
.516220+01	-.376894+02	.503415+02	.330266-01	.441647-02	-.317050-00
.610056+01	-.498806+01	-.553121+02	.441647-02	.534053-02	-.636650-01
-.752025+02	.364089+03	-.212378+03	-.317050-00	-.636650-01	.315710+01

27. CSM Covariance Matrix at Main Ascent Burnout

.718082+04	-.483381+04	-.885521+05	.423301+01	.613096+01	-.399910+02
-.483381+04	.577711+05	.792379+05	-.504871+02	-.349531+01	.502820+03
-.885521+05	.792379+05	.110813+07	-.699586+02	-.754747+02	.682047+03
.423301+01	-.504871+02	-.699586+02	.444447-01	.304460-02	-.441331-00
.613096+01	-.349531+01	-.754747+02	.304460-02	.524546-02	-.287564-01
-.399910+02	.502820+03	.682047+03	-.441331-00	-.287564-01	.441335+01

28. CSM Covariance Matrix at CSI

.774524+04	-.991670+04	-.109298+06	.860474+01	.576905+01	.638571+02
-.991670+04	.981468+05	.102302+07	-.848106+02	-.271151+01	.296751+02
-.109298+06	.102302+07	.109009+08	-.884318+03	-.417844+02	.210833+03
.860474+01	-.848106+02	-.884318+03	.732941-01	.231908-02	-.255750-01
.576905+01	-.271151+01	-.417844+02	.231908-02	.545854-02	.581924-01
.638571+02	.296751+02	.210833+03	-.255750-01	.581924-01	.694610-00

29. CSM Covariance Matrix at CD H

.751089+04	-.560094+04	.103567+06	.494111+01	.593701+01	-.239672+02
-.560094+04	.124308+06	-.100086+07	-.103938+03	-.826339+01	-.557340+03
.103567+06	-.100086+07	.873098+07	.841805+03	.104670+03	.427825+04
.494111+01	-.103938+03	.841805+03	.869970-01	.690001-02	.467767-00
.593701+01	-.826339+01	.104670+03	.690001-02	.534792-02	-.909648-02
-.239672+02	-.557340+03	.427825+04	.467767-00	-.909648-02	.302043+01

30. CSM Covariance Matrix at TPI

.747418+04	-.737389+04	.303236+05	.621168+01	.587401+01	-.938229+02
-.737389+04	.830339+05	-.665937+06	-.710625+02	-.890926+01	.406824+03
.303236+05	-.665937+06	.599836+07	.568336+03	.455481+02	-.304413+04
.621168+01	-.710625+02	.568336+03	.608816-01	.774955-02	-.347603-00
.587401+01	-.890926+01	.455481+02	.774955-02	.549158-02	-.895996-01
-.938229+02	.406824+03	-.304413+04	-.347603-00	-.895996-01	.291915+01

31. CSM Covariance Matrix at LM MCC

0.726725E 04	-0.508825E 04	-0.119898E 06	0.642286E 01	0.609082E 01	-0.284341E 02
-0.508825E 04	0.514791E 04	0.785269E 05	-0.568111E 01	-0.415847E 01	0.182363E 02
-0.119898E 06	0.785269E 05	0.201397E 07	-0.101411E 03	-0.101863E 03	0.486437E 03
0.642286E 01	-0.568111E 01	-0.101411E 03	0.660402E-02	0.525101E-02	-0.233944E-01
0.609082E 01	-0.415847E 01	-0.101863E 03	0.525101E-02	0.519108E-02	-0.247458E-01
-0.284341E 02	0.182363E 02	0.486437E 03	-0.233944E-01	-0.247458E-01	0.121626E-00

32. CSM Covariance Matrix at Rendezvous

.755672+04	-.106773+05	-.133453+06	.934864+01	.593880+01	-.695429-00
-.106773+05	.829034+05	.726971+06	-.720209+02	-.702083+01	.379834+03
-.133453+06	.726971+06	.680049+07	-.630805+03	-.100193+03	.306800+04
.934864+01	-.720209+02	-.630805+03	.626493-01	.591960-02	-.329723-00
.593880+01	-.702083+01	-.100193+03	.591960-02	.932995-02	.771513-02
-.695429-00	.379834+03	.306800+04	-.329723-00	.771513-02	.214212+01

33. CSM Covariance Matrix at TEI

0.116292E 05	-0.132330E 05	-0.125592E 05	0.107617E 02	0.562877E 01	0.135072E 03
-0.132330E 05	0.176751E 05	0.157299E 05	-0.145564E 02	-0.651490E 01	-0.153607E 03
-0.125592E 05	0.157299E 05	0.171347E 05	-0.129990E 02	-0.638173E 01	-0.151553E 03
0.107617E 02	-0.145564E 02	-0.129990E 02	0.120034E-01	0.531691E-02	0.125135E-00
0.562877E 01	-0.651490E 01	-0.638173E 01	0.531691E-02	0.277506E-02	0.659804E-01
0.135072E 03	-0.153607E 03	-0.151553E 03	0.125135E-00	0.659804E-01	0.158157E 01

34. LM Covariance Matrix at Hohmann Transfer

,644631+05	,249751+05	-,838670+06	,815057+02	-,353988+02	-,101143+03
,249751+05	,203790+05	-,478731+06	,313963+02	-,133379+02	-,896214+02
-,838670+06	-,478731+06	,131707+08	-,104966+04	,450085+03	,208423+04
,815057+02	,313963+02	-,104966+04	,106099+00	-,466032-01	-,118558+00
-,353988+02	-,133379+02	,450085+03	-,466032-01	,205678-01	,486226-01
-,101143+03	-,896214+02	,208423+04	-,118558+00	,486226-01	,440240-00

35. LM Covariance Matrix at Powered Descent

,361713+04	,662657+04	-,117542+06	-,722381+01	,827361-00	,788047+02
,662657+04	,666076+05	-,760331+06	-,846788+02	,803954+01	,869467+03
-,117542+06	-,760331+06	,945205+07	,931633+03	-,928991+02	-,945746+04
-,722381+01	-,846788+02	,931633+03	,112111+00	-,122129-01	-,114016+01
,827361-00	,803954+01	-,928991+02	-,122129-01	,322711-02	,951538-01
,788047+02	,869467+03	-,945746+04	-,114016+01	,951538-01	,121673+02

36. LM Covariance Matrix at CSI

,109610+05	-,595165+04	-,584935+05	,153879+02	-,283866+01	,104363+03
-,595166+04	,698117+04	,403175+05	-,917576+01	,234929+01	-,949831+02
-,584935+05	,403175+05	,595616+06	-,714855+02	,205399+02	-,734315+03
,153879+02	-,917576+01	-,714855+02	,224388-01	-,393841-02	,150717-00
-,283866+01	,234929+01	,205399+02	-,393841-02	,100930-02	-,364369-01
,104363+03	-,949831+02	-,734315+03	,150717-00	-,364369-01	,141697+01

37. LM Covariance Matrix at CDH

.193547+08	-.344974+08	-.686819+05	.334293+05	-.123949+05	-.246558+03
-.344974+08	.736117+08	.617627+06	-.668149+05	.224116+05	.178755+04
-.686819+05	.617627+06	.221027+07	-.523360+03	.691513+02	.251772+04
.334293+05	-.668149+05	-.523360+03	.620642+02	-.216011+02	-.150272+01
-.123949+05	.224116+05	.691513+02	-.216011+02	.796501+01	.245824-00
-.246558+03	.178755+04	.251772+04	-.150272+01	.245824-00	.719932+01

38. LM Covariance Matrix at TPI

.100876+07	-.629307+06	-.999413+05	.145364+04	-.417448+03	-.122601+03
-.629307+06	.408562+06	-.340231+05	-.908623+03	.260777+03	.554754+02
-.999413+05	-.340231+05	.862941+06	-.120267+03	.107142+02	.228543+03
.145364+04	-.908623+03	-.120267+03	.210502+01	-.607550-00	-.142824-00
-.417448+03	.260777+03	.107142+02	-.607550-00	.182442-00	.199928-02
-.122601+03	.554754+02	.228543+03	-.142824-00	.199928-02	.329578-00

39. LM Covariance Matrix at MCC

0.114249E 05	-0.284103E 04	-0.593376E 05	0.664390E 01	0.599462E 01	0.139359E 02
-0.284103E 04	0.477396E 04	0.283164E 05	-0.364259E 01	-0.180899E 01	0.142071E 02
-0.593376E 05	0.283164E 05	0.925828E 06	-0.165341E 02	-0.641527E 02	-0.166127E 03
0.664390E 01	-0.364259E 01	-0.165341E 02	0.705224E-02	0.164059E-02	-0.147090E-01
0.599462E 01	-0.180899E 01	-0.641527E 02	0.164059E-02	0.536694E-02	0.183367E-01
0.139359E 02	0.142071E 02	-0.166127E 03	-0.147090E-01	0.183367E-01	0.192180E-00

40. LM Covariance Matrix at Intercept

0.105806E 07	-0.170431E 06	-0.394216E 05	0.161199E 04	-0.264592E 03	0.411211E 02
-0.170431E 06	0.720696E 06	0.348819E 05	-0.335402E 03	0.684892E 03	-0.532619E 01
-0.394216E 05	0.348819E 05	0.118929E 07	-0.283605E 02	-0.426813E 02	0.196016E 03
0.161199E 04	-0.335402E 03	-0.283605E 02	0.247559E 01	-0.483953E-00	0.525247E-03
-0.264592E 03	0.684892E 03	-0.426813E 02	-0.483953E-00	0.682575E 00	0.522708E-01
0.411211E 02	-0.532619E 01	0.196016E 03	0.525247E-03	0.522708E-01	0.103573E 01

41. Covariance Matrix at TEI + 5 hours

.605155+07	-.928971+06	.327716+07	.470490+03	-.610968+01	.936969+02
-.928971+06	.115658+07	-.990445+07	-.770448+02	.484322+02	-.363553+03
.327716+07	-.990445+07	.964898+08	.277959+03	-.431654+03	.355026+04
.470490+03	-.770448+02	.277959+03	.375218-01	-.852934-03	.867118-02
-.610968+01	.484322+02	-.431654+03	-.852934-03	.227682-02	-.160999-01
.936969+02	-.363553+03	.355026+04	.867118-02	-.160999-01	.131055-00

42. Covariance Matrix at TEI + 10 hours

.915356+08	-.705114+08	.464407+09	.335214+04	-.174617+04	.936660+04
-.705114+08	.679206+08	-.480810+09	-.264187+04	.169316+04	-.974232+04
.464407+09	-.480810+09	.349999+10	.175637+05	-.119878+05	.710009+05
.335214+04	-.264187+04	.175637+05	.123442+00	-.655288-01	.354765-00
-.174617+04	.169316+04	-.119878+05	-.655288-01	.422486-01	-.242969-00
.936660+04	-.974232+04	.710009+05	.354765-00	-.242969-00	.144048+01

43. Covariance Matrix at TEI + 15 hours

.421647+09	-.249569+09	.137707+10	.972341+04	-.427321+04	.194986+05
-.249569+09	.156391+09	-.886878+09	-.577964+04	.268371+04	-.125796+05
.137707+10	-.886878+09	.514961+10	.319885+05	-.152075+05	.731094+05
.972341+04	-.577964+04	.319885+05	.224559-00	-.990137-01	.453236-00
-.427321+04	.268371+04	-.152075+05	-.990137-01	.460912-01	-.215755-00
.194986+05	-.125796+05	.731094+05	.453236-00	-.215755-00	.103809+01

44. Covariance Matrix at TEI + 20 hours (First MCC), Earth Reference

.191484+07	.198146+08	.335908+08	.418438+02	.271648+03	.371529+03
.198146+08	.548392+09	.267609+09	.689440+03	.841331+04	.265986+04
.335908+08	.267609+09	.189288+10	.495366+03	.172611+04	.215267+05
.418438+02	.689440+03	.495366+03	.114237-02	.103855-01	.514905-02
.271648+03	.841331+04	.172611+04	.103855-01	.132390-00	.133192-01
.371529+03	.265986+04	.215267+05	.514905-02	.133192-01	.245294-00

45. Covariance Matrix at TEI + 25 hours

.922215+06	.176486+08	-.988271+07	.210731+02	.225048+03	-.987793+02
.176486+08	.769579+09	-.615267+08	.536407+03	.953058+04	-.946701+03
-.988271+07	-.615267+08	.148557+10	-.277277+03	-.192577+04	.139628+05
.210731+02	.536407+03	-.277277+03	.538911-03	.683780-02	-.283898-02
.225048+03	.953058+04	-.192577+04	.683780-02	.118999+00	-.227750-01
-.987793+02	-.946701+03	.139628+05	-.283898-02	-.227750-01	.131470-00

46. Covariance Matrix at TEI + 30 hours

.254259+07	.489520+08	-.118539+08	.432229+02	.492899+03	-.108946+03
.489520+08	.123280+10	.147943+09	.896094+03	.121876+05	.729418+03
-.118539+08	.147943+09	.115852+10	-.181649+03	.879753+03	.906461+04
.432229+02	.896094+03	-.181649+03	.745041-03	.862070-02	-.172331-02
.492899+03	.121876+05	.879753+03	.862070-02	.120818+00	.253044-02
-.108946+03	.729418+03	.906461+04	-.172331-02	.253044-02	.711193-01

47. Covariance Matrix at TEI + 35 hours

.330355+07	.554949+08	-.129394+08	.442229+02	.463699+03	-.101618+03
.554949+08	.117017+10	.190672+09	.739090+03	.966689+04	.961983+03
-.129394+08	.190672+09	.130619+10	-.189586+03	.110786+04	.875239+04
.442229+02	.739090+03	-.189586+03	.604137-03	.618679-02	-.148420-02
.463699+03	.966689+04	.110786+04	.618679-02	.796453-01	.474054-02
-.101618+03	.961983+03	.875239+04	-.148420-02	.474054-02	.587844-01

48. Covariance Matrix at TEI + 40 hours

.238406+07	.388994+08	-.522529+07	.269683+02	.273757+03	-.410820+02
.388994+08	.794908+09	.247830+09	.423485+03	.550698+04	.123223+04
-.522529+07	.247830+09	.128138+10	-.111784+03	.140486+04	.745186+04
.269683+02	.423485+03	-.111784+03	.325114-03	.299563-02	-.787438-03
.273757+03	.550698+04	.140486+04	.299563-02	.382358-01	.665371-02
-.410820+02	.123223+04	.745186+04	-.787438-03	.665371-02	.434263-01

49. Covariance Matrix at TEI + 45 hours

.162748+07	.227799+08	.575284+07	.113115+02	.831413+02	.859140+01
.227799+08	.454076+09	.419993+09	.701102+02	.162984+04	.125292+04
.575284+07	.419993+09	.112666+10	-.111522+03	.137666+04	.365248+04
.113115+02	.701102+02	-.111522+03	.164277-03	.245595-03	-.488443-03
.831413+02	.162984+04	.137666+04	.245595-03	.589057-02	.405979-02
.859140+01	.125292+04	.365248+04	-.488443-03	.405979-02	.119622-01

50. Covariance Matrix at TEI + 50 hours

.189957+07	.252654+08	-.668099+07	.168562+02	.129564+03	-.434114+02
.252654+08	.566827+09	.370824+09	.179910+03	.278841+04	.139699+04
-.668099+07	.370824+09	.122919+10	-.128495+03	.156910+04	.538092+04
.168562+02	.179910+03	-.128495+03	.194214-03	.974647-03	-.607175-03
.129564+03	.278841+04	.156910+04	.974647-03	.139484-01	.588522-02
-.434114+02	.139699+04	.538092+04	-.607175-03	.588522-02	.236481-01

51. Covariance Matrix at TEI + 55 hours

.188490+07	.245248+08	-.128215+07	.153247+02	.107835+03	-.154357+02
.245248+08	.490767+09	.336753+09	.137924+03	.207187+04	.107270+04
-.128215+07	.336753+09	.104692+10	-.106821+03	.121378+04	.386622+04
.153247+02	.137924+03	-.106821+03	.190149-03	.667478-03	-.382334-03
.107835+03	.207187+04	.121378+04	.667478-03	.894230-02	.388511-02
-.154357+02	.107270+04	.386622+04	-.382334-03	.388511-02	.143719-01

52. Covariance Matrix at TEI + 60 hours

.170853+07	.225881+08	.495383+07	.123460+02	.838261+02	.817921+01
.225881+08	.440886+09	.398897+09	.817733+02	.156345+04	.110764+04
.495383+07	.398897+09	.110245+10	-.110288+03	.124321+04	.340232+04
.123460+02	.817733+02	-.110288+03	.187857-03	.377625-03	-.268343-03
.838261+02	.156345+04	.124321+04	.377625-03	.571361-02	.352789-02
.817921+01	.110764+04	.340232+04	-.268343-03	.352789-02	.106270-01

53. Covariance Matrix at TEI + 65 hours

.217468+07	.199897+08	.301649+07	.106633+02	.606601+02	-.280987+01
.199897+08	.264733+09	.306829+09	.251612+02	.752833+03	.640477+03
.301649+07	.306829+09	.119886+10	-.151997+03	.729628+03	.299974+04
.106633+02	.251612+02	-.151997+03	.198408-03	.151806-03	-.253548-03
.606601+02	.752833+03	.729628+03	.151806-03	.226984-02	.158856-02
-.280987+01	.640477+03	.299974+04	-.253548-03	.158856-02	.773391-02

54. Covariance Matrix at TE MCC 2 (TEI + 70 hours)

.112848+07	.944174+07	.146910+08	.416079+01	.226854+02	.276844+02
.944174+07	.160812+09	.342612+09	-.518939+02	.315421+03	.582897+03
.146910+08	.342612+09	.982520+09	-.965620+02	.634370+03	.187702+04
.416079+01	-.518939+02	-.965620+02	.199072-03	-.104294-05	.890446-04
.226854+02	.315421+03	.634370+03	-.104294-05	.690639-03	.120132-02
.276844+02	.582897+03	.187702+04	.890446-04	.120132-02	.411889-02

55. Covariance Matrix at TEI + 75 hours

.143557+07	.109785+08	-.748079+06	.431504+01	.162051+02	-.105069+02
.109785+08	.164606+09	.223443+09	-.905373+02	.189104+03	.401883+02
-.748079+06	.223443+09	.948674+09	-.261264+03	.142803+03	.818419+03
.431504+01	-.905373+02	-.261264+03	.324535-03	-.112799-04	.810310-04
.162051+02	.189104+03	.142803+03	-.112799-04	.326964-03	.603194-04
-.105069+02	.401883+02	.818419+03	.810310-04	.603194-04	.116090-02

56. Covariance Matrix at TEI + 80 hours

.115989+07	.893204+07	.982666+06	-.121038+01	.137197+01	-.150429+02
.893204+07	.140924+09	.201776+09	-.164070+03	-.195871+02	-.290426+03
.982666+06	.201776+09	.834000+09	-.341352+03	-.122589+03	-.343167+03
-.121038+01	-.164070+03	-.341352+03	.465279-03	.104702-03	.595693-03
.137197+01	-.195871+02	-.122589+03	.104702-03	.998997-04	.162746-03
-.150429+02	-.290426+03	-.343167+03	.595693-03	.162746-03	.851991-03

57. Covariance Matrix at TEI + 85 hours

.312096+07	.213292+08	.252958+08	-.158420+02	-.437242+02	-.102535+03
.213292+08	.177509+09	.207972+09	-.202931+03	-.358314+03	-.874217+03
.252958+08	.207972+09	.545883+09	-.156492+03	-.440282+03	-.135649+04
-.158420+02	-.202931+03	-.156492+03	.522528-03	.455928-03	.117924-02
-.437242+02	-.358314+03	-.440282+03	.455928-03	.803568-03	.192077-02
-.102535+03	-.874217+03	-.135649+04	.117924-02	.192077-02	.494248-02

58. Covariance Matrix at TEI + 90 hours

.518579+07	.181143+08	.373514+08	-.196187+02	-.971114+02	-.314443+03
.181143+08	.908478+08	.102069+09	-.208861+03	-.468245+03	-.117375+04
.373514+08	.102069+09	.440545+09	-.518258+02	-.569465+03	-.295975+04
-.196187+02	-.208861+03	-.518258+02	.102105-02	.106731-02	.234151-02
-.971114+02	-.468245+03	-.569465+03	.106731-02	.246560-02	.641402-02
-.314443+03	-.117375+04	-.295975+04	.234151-02	.641402-02	.244122-01

59. Covariance Matrix at TEI + 95 hours

.385658+07	.106092+08	.826927+07	-.453501+02	-.220097+03	-.455460+03
.106092+08	.424210+08	.600976+07	-.275500+03	-.832312+03	-.114790+04
.826927+07	.600976+07	.112857+09	.119710+03	-.171708+03	-.237795+04
-.453501+02	-.275500+03	.119710+03	.245553-02	.522697-02	.439250-02
-.220097+03	-.832312+03	-.171708+03	.522697-02	.165066-01	.242116-01
-.455460+03	-.114790+04	-.237795+04	.439250-02	.242116-01	.786292-01

60. Covariance Matrix at Entry

.569258+05	-.139444+05	-.366909+05	.522282+01	-.224495+02	-.368013+03
-.139444+05	.512517+06	-.255866+05	-.421564+03	-.607286+02	.812139+03
-.366909+05	-.255866+05	.153506+06	.367299+02	.271140+01	-.173890+03
.522282+01	-.421564+03	.367299+02	.349480-00	.496519-01	-.625982-00
-.224495+02	-.607286+02	.271140+01	.496519-01	.230626-01	.313704-01
-.368013+-3	.812139+03	-.173890+03	-.625982-00	.313704-01	.577202+01

TABLE A-II.- A PRIORI COVARIANCE MATRICES

(a) Covariance Matrix at TLI Cut-off

$$\begin{bmatrix} 0.999128E07 & 0.136163E08 & 0.262707E07 & 0.117286E05 & -0.978271E04 & 0.955288E04 \\ & 0.721274E08 & 0.911758E07 & -0.741309E05 & -0.387388E04 & 0.293625E05 \\ & & 0.481817E07 & -0.959030E04 & -0.480759E04 & 0.275409E05 \\ \text{Symmetrical} & & & 0.230696E03 & -0.377761E02 & -0.348020E02 \\ & & & & 0.173383E02 & -0.293429E02 \\ & & & & & 0.173574E03 \end{bmatrix}$$

(b) Covariance Matrix at Lunar Deboost Cut-off

$$\begin{bmatrix} 0.327210E07 & -0.716502E07 & 0.102069E08 & 0.551016E04 & 0.116226E04 & -0.178659E05 \\ & 0.365747E08 & -0.321242E08 & -0.238183E05 & -0.326450E04 & 0.530471E05 \\ & & 0.456192E08 & 0.193995E05 & 0.619134E04 & -0.750014E05 \\ \text{Symmetrical} & & & 0.236029E02 & 0.258471E01 & -0.312345E02 \\ & & & & 0.741135E01 & -0.102614E02 \\ & & & & & 0.136618E03 \end{bmatrix}$$

(c) Covariance Matrix at TEI Cut-off

$$\begin{bmatrix} 0.233478E06 & 0.732836E05 & 0.994843E05 & 0.172098E04 & 0.803423E03 & 0.137924E04 \\ & 0.693803E06 & -0.436870E05 & 0.939781E02 & 0.114827E04 & 0.139539E02 \\ & & 0.571698E05 & 0.769867E03 & 0.263830E03 & 0.746678E03 \\ \text{Symmetrical} & & & 0.133022E02 & 0.532453E01 & 0.102823E02 \\ & & & & 0.511770E01 & 0.454752E01 \\ & & & & & 0.104112E02 \end{bmatrix}$$

REFERENCES

1. Mission Analysis Branch: AS-504A Preliminary Spacecraft Reference Trajectory, Volumes I and II (U). MSC Internal Note No. 66-FM-70, July 1, 1966.

2. GSFC and MSC: Apollo Navigation Working Group Technical Report No. 66-AN-1.1, April 4, 1966.

3. GSFC and MSC: Apollo Navigation Working Group Technical Report No. 66-AN-2.1, Sept. 1, 1966.

4. Mitchell, Paul H.: Position and Velocity Uncertainties at Translunar Injection. MSC Internal Note No. 66-FM-114, Oct. 14, 1966.

5. Mitchell, Paul H.: An Error Analysis of Cislunar Flight. MSC Internal Note No. 66-FM-37, April 6, 1966.